

Article

Not peer-reviewed version

In Vitro and *In Silico* Analyses Explore the Role of Flavonoid Classes in the Antiviral Activity of Plant Extracts Against the Dengue Virus

[Sindi Alejandra Velandia](#) , [Elena E Stashenko](#) , [Elizabeth Quintero-Rueda](#) , [Sergio Conde-Ocacionez](#) ,
Lady Johanna Sierra , [Raquel E Ocacionez](#) *

Posted Date: 23 October 2025

doi: [10.20944/preprints202510.1831.v1](https://doi.org/10.20944/preprints202510.1831.v1)

Keywords: dengue virus; dengue treatment; plant extracts; flavonoids



Preprints.org is a free multidisciplinary platform providing preprint service that is dedicated to making early versions of research outputs permanently available and citable. Preprints posted at Preprints.org appear in Web of Science, Crossref, Google Scholar, Scilit, Europe PMC.

Copyright: This open access article is published under a Creative Commons CC BY 4.0 license, which permit the free download, distribution, and reuse, provided that the author and preprint are cited in any reuse.

Disclaimer/Publisher's Note: The statements, opinions, and data contained in all publications are solely those of the individual author(s) and contributor(s) and not of MDPI and/or the editor(s). MDPI and/or the editor(s) disclaim responsibility for any injury to people or property resulting from any ideas, methods, instructions, or products referred to in the content.

Article

In Vitro and In Silico Analyses Explore the Role of Flavonoid Classes in the Antiviral Activity of Plant Extracts Against the Dengue Virus

Sindi Alejandra Velandia ¹, Elena E Stashenko ¹, Elizabeth Quintero-Rueda ¹, Sergio Conde-Ocacionez ², Lady Johanna Sierra ¹ and Raquel E Ocacionez ^{1,*}

¹ Research Center for Chromatography and Mass Spectrometry (CROM-MASS), Universidad Industrial de Santander, Carrera 27, Calle 9, Bucaramanga 680002, Colombia

² Netherlands Institute for Neuroscience, Royal Netherlands Academy of Arts and Sciences UMC location University of Amsterdam, Amsterdam, The Netherlands

* Correspondence: relocaz@uis.edu.co

Abstract

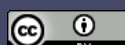
This study aimed to determine the association between the content of flavonoids and antiviral effect of plant extracts against the dengue virus (DENV). Extracts from medicinal plants cultivated in Colombia were prepared by ultrasonic-assisted solvent extraction (UAE) and supercritical fluid extraction (SFE). UHPLC/ESI-Q-Orbitrap-MS analysis identified forty-six flavonoids. Fourteen extracts were tested for their ability to reduce the cytopathic effect (CPE) induced by DENV in Vero cells. UAE extracts of *Scutellaria coccinea*, *Scutellaria incarnata*, and *Lippia alba* contained higher amounts of flavonoid glycosides (from 97.0% to 87.9%) rather than aglycones, and effectively reduced CPE- DENV (IC_{50} : 3.0 to 65 μ g/mL; SI: 0.4 to 71). UAE and SFE extracts from *L. origanoides* with higher content of aglycones (41.7% to 93.4%) than glycosides (0.0 to 58.3%) did not reduce the CPE- DENV. Cluster and one-way ANOVA analyses indicated that strong antiviral effect is associated with increased levels of flavone glycosides in the extract. Docking analyses (AutoDock Vina) revealed that flavonoid glycosides exhibited better binding affinity to target proteins (E, Gas6-Axl, clathrin, and dynamin) than aglycones. This study establishes a scientific basis for using extracts rich in flavonoid glycosides, particularly flavones, as starting points for developing plant-based therapies to treat dengue.

Keywords: dengue virus; dengue treatment; plant extracts; flavonoids

1. Introduction

Dengue virus (DENV) causes a spectrum of disease ranging from asymptomatic infection to dengue fever and severe dengue shock syndrome [1]. According to the Pan American Health Organization, dengue fever increased significantly in the Americas in 2024 rising by 232% compared to 2023 and 421% compared to the average of the previous five years [2]. There are currently no specific antiviral treatments for dengue, so therapy is primarily supportive [3]. Although two vaccines have been approved in some countries, their use is constrained due to safety concerns and their limited effectiveness against all DENV serotypes [4]. Dengue is a complex disease, making the discovery of effective therapies challenging. Increasing evidence suggests that herbal medicines have the potential as sources for clinical dengue treatments [5]. Administration of such medicines after virus exposure has shown to reduce the risk of severe dengue [5,6]. Thus, analyzing plant extracts has become an important strategy to discover and develop alternative therapies for dengue [5,7].

Plant-derived extracts prepared from a variety of species cultivated in different countries have demonstrated antiviral properties against human viruses, including DENV [5–7]. Their antiviral effect varies according to the plant species, chemotype, and phenological stages. The chemical



composition of plant extracts depends on both the species and the extraction technique used which, in turn, affects their antiviral activity [7–9]. Diverse secondary metabolites, especially phenolic compounds such as flavonoids, have shown the potential to inhibit a variety of human pathogenic viruses, including influenza H1N1, HIV, and Zika [7–9]. Further research is necessary to fully elucidate chemical profiles that explain the anti-DENV activity of plant extracts. Studies demonstrate that plant-derived flavonoids have antiviral properties and can inhibit DENV by interfering with viral replication, entry, or specific viral proteins [10,11].

The genus *Scutellaria* (Lamiaceae) includes about 400 species widely distributed across America, Europe and Asia [12]. *S. baicalensis* is recognized as a promising natural source of compounds for treating viral diseases [13]. The genus *Lippia* (Verbenaceae) comprises 150 species, primarily found in the Americas, tropical Africa and India [14]. *Lippia alba* (Mill.) N.E. Brown was the first plant approved by the French Medicines Agency for inclusion in the French Pharmacopoeia [15]. *L. origanoides* Kunth was included in the *Formulário de Fitoterápicos da Farmacopéia Brasileira* due to its strong antibacterial properties [16]. *L. alba* and *L. origanoides* are traditionally used to treat viral infections such as influenza, measles and gastroenteritis [17,18]. Extracts prepared from *S. baicalensis* and *L. origanoides* have demonstrated inhibitory effect on the replication of DENV and other enveloped viruses [19,20]. We have investigated biological activities of both *Lippia* species and *Scutellaria* species cultivated in Colombia, and their extract chemical composition have been documented [20–24].

Dengue has been identified as a significant and persistent public health concern in Colombia, which is among one of the most affected countries in the Americas. From 2012 to 2020, annual incidence rate ranged from 90.7 to 476.2 per 100,000 population, with the most recent outbreak reported in 2019 (465.9 per 100,000 population) [25]. Traditional Colombian herbal remedies are widely used to alleviate dengue symptoms, although few plants have been systematically studied for their therapeutic potential [26]. Research on the anti-DENV activity of plant extracts contributes to discovering alternative therapies to prevent severe dengue. In this study, we evaluated the *in vitro* anti-DENV activity of extracts from *Scutellaria* species and *L. alba* and *L. origanoides* and investigated the influence of their flavonoid content. *In silico* analyses were also performed to hypothesize how flavonoid in the extracts might interfere with DENV entry into Vero cells.

2. Results

2.1. Cytotoxicity

Fourteen extracts from *Scutellaria*, *L. alba*, and *L. origanoides* were selected for analysis, including eight prepared in this study and six in previous studies [20–22]. The characteristics of the extracts are summarized in Table 1, categorized by plant species, chemotype, and extraction technique. Eleven extracts were prepared using ultrasound-assisted extraction (UAE) at different temperatures (50 °C and 47 °C) and extraction time (60, 23, and 15 minutes). Three extracts from *L. origanoides* were prepared using supercritical fluid extraction (SFE).

Table 1. Extracts include in the study.

Plant	Voucher	Extract code	Extraction	
			Technique	Conditions
<i>Scutellaria coccinea</i> Kunth	UIS219784	ScSE	UAE	15 min; 50 °C
<i>Scutellaria incarnata</i> Vent	UIS219783	SiSE1	UAE	5 min; 50 °C
		SiSE2	UAE	60 min; 50 °C
<i>Scutellaria ventenatii</i> + <i>incarnata</i> (hybrid)	UIS219785	SviSE	UAE	60 min; 50 °C
<i>Lippia alba</i> (Mill) N.E. Brown	UIS22031 ^a	LacSE	UAE	60 min; 50 °C
	UIS22002 ^b	LaiSE	UAE	60 min; 50 °C
		LopSE1	UAE	23 min; 47 °C
<i>Lippia origanoides</i> Kunth	UIS22035 ^c	LopSE2	UAE	60 min; 50 °C
		LopSFE	SFE	96 min; 307 bar
	UIS22034 ^d	LocSE1	UAE	23 min; 47 °C

UIS19799 ^e	LocSE2	UAE	60 min; 50 °C
	LocSFE	SFE	96 min; 307 bar
	LotSE	UAE	23 min; 47 °C
	LotSFE	SFE	96 min; 307 bar

Lippia chemotypes are based on the major components of their essential oils. ^a Carvone, ^b citral, ^c phellandrene, ^d carvacrol, and ^e thymol. UAE, ultrasound assisted solvent extraction. SFE, supercritical fluid extraction. The following extracts were prepared in previous studies: ScSE and SiSE1 [22]; LopSE1 [20]; and LopSFE, LocSFE and LotSFE [21].

Cytotoxicity of the extracts was assessed in Vero cells uninfected with DENV using crystal violet assays. Assays were carried out at corresponding time points as the antiviral assay to determine non-cytotoxic concentrations for the cell. All extracts were non-toxic at 100 µg/mL, the maximum concentration used for antiviral assays (Figure 1A). Additional assays following the standard protocol determined the 50% cytotoxicity concentration (CC₅₀). Extracts from *Scutellaria* and *L. alba*, along with two extracts from *L. origanoides* (LopSE1 and LocSE2) reduced cell viability with CC₅₀ values ranging from 23 µg/mL to 213 µg/mL (Figure 1B). The extract from *S. ventenatii* + *incarnata* (SivSE) and one extract from *S. incarnata* (SiSE1) exhibited the highest cytotoxicity (CC₅₀: 23 and 50 µg/mL). The remaining six *L. origanoides* extracts showed no cytotoxicity at the maximum concentration tested, suggesting CC₅₀ values greater than 250 µg/mL.

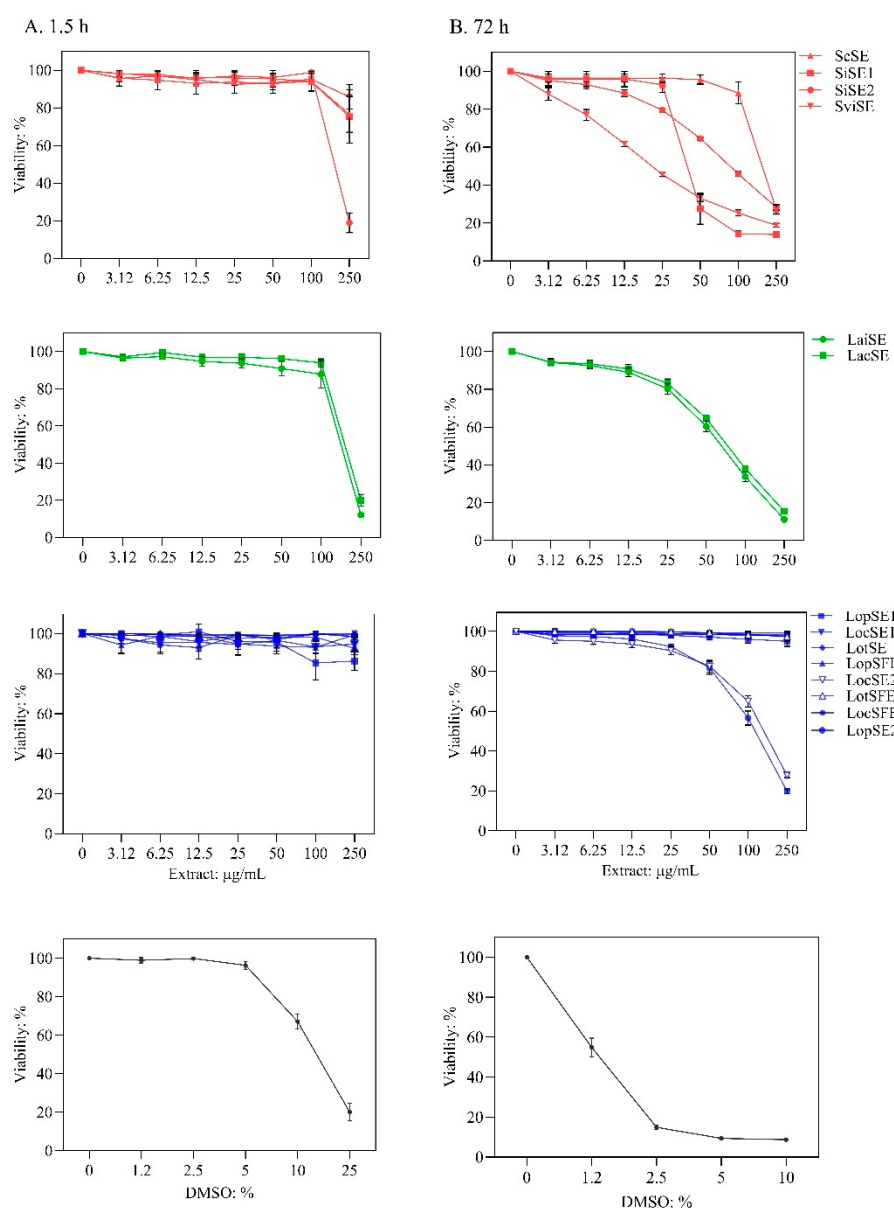


Figure 1. Cytotoxicity of the extracts in the crystal violet assay. **A.** Vero cells were treated with extract for 1.5 h, after which the extract was removed. Cell viability was measured five days after treatment. **B.** Cells were cultured in medium containing the extract for 72 h, after which the viability was measured. *S. coccinea* (ScSE), *S. incarnata* (SiSE1 and SiSE2) and *S. venentatti + incarnata* (SviSE); *L. alba* carvone (LacSE) and citral (LaiSE) chemotypes; and *L. origanoides* phellandrene (LopSE1, LopSE2, LopSFE), carvacrol (LocSE1, LocSE2, LocSFE) and thymol (LotSE, LotSFE) chemotypes. Dimethylsulfoxide (DMSO) was used as the positive control. Data are presented as mean \pm SD of six measurements from three independent analyses.

2.2. Antiviral Effect

Virus-induced cytopathic effect (CPE) is a surrogate measure of virus replication *in vitro*; therefore, lower DENV-induced CPE indicates stronger antiviral activity [27]. The extracts were tested at six nontoxic concentrations to evaluate their effect on CPE caused by DENV-1 and DENV-2 after treatment during virus adsorption to Vero cells. The presence of DENV in untreated cells was confirmed by detection of non-structural protein 1 (NS1 = 75 ± 1.97 PanBio units) using an ELISA kit. Antiviral effects were classified as: (i) strong, greater than 50% reduction in CPE of both virus serotypes with IC_{50} values lower than 55 μ g/mL; (ii) weak, $IC_{50} \leq 55$ μ g/mL for only one serotype or IC_{50} between 55 and 100 μ g/ml for one or both serotypes; and (iii) inactive, no significant CPE reduction in either serotype. Selectivity index (SI) was included in the analysis; extract with $IC_{50} \leq 55$ μ g/mL and $SI \geq 3.0$ was considered as promising anti-DENV sample. The extracts exhibited variable anti-DENV effect and selectivity (Figure 2 and Table 2).

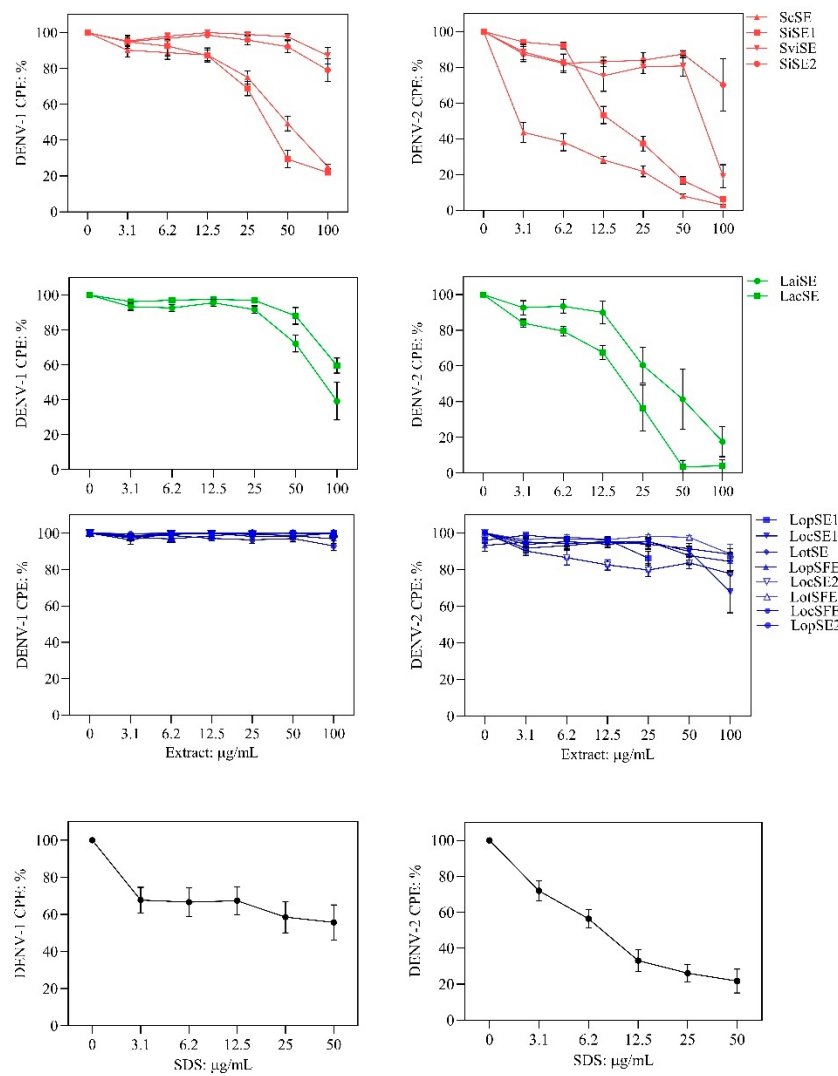


Figure 2. Antiviral effect of the extracts against dengue virus (DENV-1 and DENV-2) in the cytopathic effect (CPE)-based assay. Extracts were added during virus adsorption to Vero cells. Quantification of crystal violet staining was performed to indirectly measure virus-induced CPE. DENV- CPE %: [(OD₅₇₀ of virus-infected and extract-treated cells / OD₅₇₀ of non-infected non-treated cells)]. Scutellaria species (red), L. alba (green) and L. organoides (blue) extracts. Sodium dodecyl sulfate (SDS) is an antiviral agent. Data are presented as mean ± SD of six measurements from three independent analyses.

Table 2. Antiviral effect of the extracts on DENV-infected Vero cells.

Extract Code	CC ₅₀ : µg/mL	DENV-1			DENV-2			Effect
		CPE %	IC ₅₀ : µg/mL	SI	CPE: %	IC ₅₀ : µg/mL	SI	
ScSE ^a	213 ± 1.1	25 ± 1.2	52 ± 1.3	4.1	2.9 ± 0.45	3 ± 1.3	71	Strong
SiSE1 ^a	50 ± 1.2	22 ± 1.4	39 ± 1.2	1.2	6.1 ± 0.97	17 ± 1.2	2.9	Strong
SiSE2 ^a	91 ± 1.05	79 ± 6.5	-	-	70 ± 14.7	-	-	Inactive
SviSE ^a	23 ± 2.0	87 ± 4.7	-	-	19 ± 6.5	65 ± 1.2	0.4	Weak
LaiSE ^b	65 ± 1.1	39 ± 10.8	81 ± 1.1	0.8	17 ± 8.4	38 ± 1.2	1.7	Weak
LacSE ^b	75 ± 1.0	60 ± 4.3	-	-	4 ± 3.7	19 ± 1.1	3.9	Weak
LopSE1 ^c	>250.0	100	-	-	86 ± 3.7	-	-	Inactive
LopSE2 ^c	117 ± 1.0	93 ± 2.7	-	-	77 ± 8.4	-	-	Inactive
LopSFE ^c	>250.0	100	-	-	94 ± 3.2	-	-	Inactive
LocSE1 ^c	>250.0	100	-	-	67 ± 11.2	-	-	Inactive
LocSE2 ^c	143 ± 1.1	100	-	-	88 ± 3.2	-	-	Inactive
LocSFE ^c	>250.0	96 ± 2.5	-	-	96 ± 2.0	-	-	Inactive
LotSE ^c	>250.0	100	-	-	84 ± 4.9	-	-	Inactive
LotSFE ^c	>250.0	99 ± 0.2	-	-	88 ± 5.2	-	-	Inactive

^a *Scutellaria*, ^b *L. alba*, and ^c *L. organoides* extracts. CC₅₀ >250 µg/mL was adopted for extracts that did not exhibit a 50% reduction in cell viability (Figure 1B). CPE %: percentage of virus-induced cytopathic effect after treatment with 100 µg/mL relative to the untreated control (100% CPE). SI, selectivity index (CC₅₀ / IC₅₀).

Extracts from *S. coccinea* (ScSE) and *S. incarnata* (SiSE1) exhibited strong anti-DENV effect. ScSE showed IC₅₀ values < 53 µg/mL and SI values > 4.0, indicating promising anti-DENV sample. SiSE1 showed IC₅₀ values < 40 µg/mL, but SI values < 3.0, suggesting reduced antiviral promise. The other *S. incarnata* extract (SiSE2) was inactive, significant reduction of the virus-induced CPE of both serotypes was not detected. The *S. venentatti + incarnata* (SviSE) extract exhibited weak antiviral effect, reduced DENV-2 at IC₅₀ of 65 µg/mL (SI of 0.4), but not DENV-1. Extracts from *L. alba* exhibited weak antiviral effect. LaiSE (citral chemotype) reduced the replication of both virus serotypes, but at IC₅₀ of 81 µg/mL against DENV-1. LacSE (carvone chemotype) showed antiviral promise against DENV-2 (IC₅₀ of 19 µg/mL and SI of 3.9), but was inactive against DENV-1. All eight extracts from *L. organoides* were inactive against both virus serotypes.

2.3. UHPLC/ESI-Q-Orbitrap-MS Analysis of the Extracts Prepared in This Study

The analysis, based on retention times (R_t) and fragmentation patterns, identified only compounds belonging to the flavonoid class, including glycosides (n = 19), aglycones (n = 19) and methylated (n = 3) (Tables 3 and 4).

Table 3. Flavonoids in the extracts prepared in the study identified by UHPLC/ESI-Q-Orbitrap-MS.

Name	Formula	Exp. Masses [M+H] ⁺	Δ ppm	HCD, eV	Product ions			References
					Fragment type	Formula	(m/z)	
Apigenin-7-glucoside	C ₂₁ H ₂₀ O ₁₀	433.11287	0.11	30	[(M+H)-C ₆ H ₁₀ O ₅] ⁺ [(M+H)-C ₆ H ₁₀ O ₅ -H ₂ O] ⁺ [(M+H)-C ₆ H ₁₀ O ₅ -CO] ⁺	C ₁₅ H ₁₁ O ₅ C ₁₅ H ₉ O ₄ C ₁₄ H ₁₁ O ₄	271.06012 253.04997 243.06558	[19,22]

					$[(M+H)-C_6H_{10}O_5-C_8H_6O]^+$	$C_7H_5O_4$	153.01848
					$[(M+H)-C_6H_{10}O_5-C_8H_6O_3]^+$	$C_7H_5O_2$	121.02852
Apigenin-7-glucuronide	$C_{21}H_{18}O_{11}$	447.09056	0.54	20	$[(M+H)-C_6H_8O_6]^+$ $[(M+H)-C_6H_8O_6-C_8H_6]^+$	$C_{15}H_{11}O_5$ $C_7H_5O_5$	271.06033 169.01256
Baicalin	$C_{21}H_{18}O_{11}$	447.09056	0.33	20	$[(M+H)-C_6H_8O_6]^+$ $[(M+H)-C_6H_8O_6-C_8H_6]^+$	$C_{15}H_{11}O_5$ $C_7H_5O_5$	271.06033 169.01256
Chrysoeriol-7-diglucuronide	$C_{28}H_{28}O_{18}$	653.13484	0.50	20	$[(M+H)-C_6H_8O_6]^+$ $[(M+H)-2C_6H_8O_6]^+$	$C_{22}H_{21}O_{12}$ $C_{16}H_{13}O_6$	477.10275 301.07066
Chrysoeriol-7-glucuronide	$C_{22}H_{20}O_{12}$	477.10275	0.20	20	$[(M+H)-C_6H_8O_6]^+$	$C_{16}H_{13}O_6$	301.07066
Dihydrobaicalein-glucuronide	$C_{21}H_{20}O_{11}$	449.10602	0.44	10	$[(M+H)-C_6H_8O_6]^+$ $[(M+H)-C_6H_8O_6-C_8H_8]^+$ $[(M+H)-C_6H_8O_6-C_6H_6O_4]^+$	$C_{15}H_{13}O_5$ $C_7H_5O_5$ C_9H_7O	273.07538 169.01341 131.04932
Eriodictyol-7-glucoside	$C_{21}H_{22}O_{11}$	451.12327	0.48	10	$[(M+H)-C_6H_{10}O_5]^+$ $[(M+H)-C_6H_{10}O_5-H_2O]^+$ $[(M+H)-C_6H_{10}O_5-C_8H_8O_2]^+$	$C_{15}H_{13}O_6$ $C_{15}H_{11}O_5$ $C_7H_5O_4$	289.07062 271.05969 153.01810
Luteolin-7-glucuronide	$C_{21}H_{18}O_{12}$	463.08710	1.57	30	$[(M+H)-C_6H_7O_6]^+$ $[(M+H)-C_6H_7O_6-H_2O]^+$	$C_{21}H_{17}O_{12}$ C_{20} $^{13}CH_{17}O_{12}$ $C_{21}H_{17}O_{11}$	461.07211 462.07553 463.07739
^{18}O							
Eriodictyol-rhamnoside	$C_{21}H_{22}O$	435.128	0.28	3	$[(M+H)-C_6H_{10}O_4]^+$ $[(M+H)-C_6H_{10}O_4-H_2O]^+$ $[(M+H)-C_6H_{10}O_4-H_2O-C_6H_4O_2]^+$ $[(M+H)-C_6H_{10}O_4-C_8H_8O_2]^+$	$C_{15}H_{13}O$ $C_{15}H_{11}O$ $C_9H_7O_3$ $C_7H_5O_4$	86 37 163.038 153.018
Galangin	$C_{21}H_{20}O$	433.112	0.11	2	$[(M+H)-C_6H_{10}O_5]^+$ $[(M+H)-C_6H_{10}O_5-C_2H_2O]^+$ $[(M+H)-C_6H_{10}O_5-C_6H_4O_2]^+$ $[(M+H)-C_6H_{10}O_5-C_8H_6O]^+$	$C_{15}H_{11}O$ $C_{13}H_9O_4$ $C_9H_7O_3$ $C_7H_5O_4$	12 35 163.038 153.018
Luteolin-7-glucoside	$C_{21}H_{20}O$	449.107	1.07	2	$[(M+H)-C_6H_{10}O_5]^+$ $[(M+H)-C_6H_{10}O_5-C_2H_2O]^+$ $[(M+H)-C_6H_{10}O_5-C_6H_4O_2]^+$ $[(M+H)-C_6H_{10}O_5-C_8H_6O_2]^+$	$C_{15}H_{11}O$ $C_{13}H_9O_5$ $C_9H_7O_4$ $C_7H_5O_4$	15 86 179.034 153.018

							449.108
Luteolin							
- rutinoside	C ₂₇ H ₃₀ O	595.165	0.86	1	[(M+H)-C ₆ H ₁₀ O ₄] ⁺	C ₂₁ H ₂₁ O	64
de		15	24	0	[(M+H)-C ₆ H ₁₀ O ₄ -C ₆ H ₁₀ O ₅] ⁺	11	287.055
					[(M+H)-C ₆ H ₁₀ O ₄ -C ₆ H ₁₀ O ₅ -C ₈ H ₆ O ₂] ⁺	C ₁₅ H ₁₁ O	30
						6	153.018
					[(M+H)-C ₆ H ₁₀ O ₄ -C ₆ H ₁₀ O ₅ -C ₈ H ₆ O ₃] ⁺	C ₇ H ₅ O ₄	32
						C ₇ H ₅ O ₃	137.023
							25
Phloridzin	C ₂₁ H ₂₄ O	437.143	0.82	1	[(M+H)-C ₆ H ₁₀ O ₅] ⁺	C ₁₅ H ₁₅ O	275.091
		10	86	0	[(M+H)-C ₆ H ₁₀ O ₅ -H ₂ O] ⁺	5	31
					[(M+H)-C ₆ H ₁₀ O ₅ -C ₇ H ₆ O] ⁺	C ₁₅ H ₁₃ O	257.080
						4	[20,31]
						C ₈ H ₉ O ₄	169.049
							61
							303.049
Quercetin-3-glucoside	C ₂₁ H ₂₀ O	465.102	0.35	1	[(M+H)-C ₆ H ₁₀ O ₅] ⁺	C ₁₅ H ₁₁ O	71
		12	87	0	[(M+H)-C ₆ H ₁₀ O ₅ -H ₂ O] ⁺	7	285.039
					[(M+H)-C ₆ H ₁₀ O ₅ -C ₈ H ₆ O ₃] ⁺	C ₁₅ H ₉ O ₆	70
						C ₇ H ₅ O ₄	[20]
							153.018
							11
Scutellarin	C ₂₁ H ₁₈ O	463.087	0.42	1	[(M+H)-C ₆ H ₈ O ₆] ⁺	C ₁₅ H ₁₁ O	287.055
		12	62	0	[(M+H)-C ₆ H ₈ O ₆ -C ₆ H ₄ O ₃] ⁺	6	37
						C ₉ H ₇ O ₃	[22]
							163.038
							85
Taxifolin-7-glucoside	C ₂₁ H ₂₂ O	467.118	0.24	2	[(M+H)-C ₆ H ₁₀ O ₅] ⁺	C ₁₅ H ₁₃ O	305.065
		12	29	0	[(M+H)-C ₆ H ₁₀ O ₅ -H ₂ O] ⁺	7	61
					[(M+H)-C ₆ H ₁₀ O ₅ -C ₈ H ₈ O ₃] ⁺	C ₁₅ H ₁₁ O	287.054
						6	[20]
						C ₇ H ₅ O ₄	153.018
							32
Tricin-7-diglucuronoside	C ₂₉ H ₃₀ O ₁₉	683.145	0.28	30	[(M+H)-C ₆ H ₈ O ₆] ⁺	C ₂₃ H ₂₃ O ₁₃	[31,32]
			40		[(M+H)-2C ₆ H ₈ O ₆] ⁺	C ₁₇ H ₁₅ O ₇	507.11331
							331.08122
Tricin-glucuronide	C ₂₃ H ₂₂ O ₁₃	507.113	1.03	20	[(M+H)-C ₆ H ₈ O ₆] ⁺	C ₁₇ H ₁₅ O ₇	[31,32]
		31					331.08063
Wogonoside	C ₂₂ H ₂₀ O ₁₁	461.177	0.47	20	[(M+H)-C ₆ H ₈ O ₆] ⁺	C ₁₆ H ₁₃ O ₅	285.07535
			73		[(M+H)-C ₆ H ₈ O ₆ -C _{H3}] ⁺	C ₁₅ H ₁₀ O ₅	[22]
							270.05164

Acacetin	$C_{16}H_{12}$ O ₅	285.075 41	1.19	50	$[(M+H)-CH_3]^{+•}$	C ₁₅ H ₁₀	270.05273	[30, 31]
					$[(M+H)-CH_3-CO]^{+•}$	O ₅	242.05754	
					$[(M+H)-C_9H_8O]^+$	C ₁₄ H ₁₀	153.01842	
					$[(M+H)-C_8H_6O_4]^+$	O ₄	119.04922	
						C ₇ H ₅ O ₄	8	
Apigenin	$C_{15}H_{10}$ O ₅	271.060 42	0.82	40	$[(M+H)-H_2O]^+$	C ₁₅ H ₉ O	253.04997	[21, 22]
					$[(M+H)-CO]^+$	C ₁₄ H ₁₁	243.06558	
					$[(M+H)-C_8H_6O]^+$	O ₄	153.01848	
Baicalein	$C_{15}H_{10}$ O ₅	271.059 69	1.50	60	$[(M+H)-H_2O]^+$	C ₇ H ₅ O ₄		
					$[(M+H)-H_2O-CO]^+$	C ₁₅ H ₉ O	253.04919	
					$[(M+H)-C_8H_6]^+$	C ₁₄ H ₉ O	225.05435	
					$[(M+H)-C_8H_6-CO]$	C ₇ H ₅ O ₅	169.01305	[19,
					$+ [M+H]-C_8H_6-CO$	C ₆ H ₅ O ₄	141.01811	22]
					$-H_2O]^+$	C ₆ H ₃ O ₃	123.00773	
					$[(M+H)-C_7H_4O_5]^+$	C ₈ H ₇	103.04451	
Chrysoerio 1	$C_{16}H_{12}$ O ₆	301.070 36	0.99	30	$[(M+H)-CH_3]^{+•}$	C ₁₅ H ₁₀	286.04718	[20, 21]
					$[(M+H)-CH_3-CO]^{+•}$	C ₁₄ H ₁₀	258.05222	
					$[(M+H)-C_9H_8O_2]^+$	O ₅	153.01855	
					$[(M+H)-C_7H_4O_4]^+$	C ₇ H ₅ O ₄	149.05977	
					$[(M+H)-C_8H_6O_5]^+$	C ₉ H ₉ O ₂	119.04939	
Cirsimari n	$C_{17}H_{14}$ O ₆	315.086 05	0.83	30	$[(M+H)-CH_3]^{+•}$	C ₈ H ₇ O		
					$[(M+H)-2CH_3]^{+•}$	C ₁₆ H ₁₂	300.06265	
					$[(M+H)-CH_3-H_2O]$	C ₁₅ H ₉ O	285.03961	
					$+ [M+H]-CH_3-H_2O$	C ₁₆ H ₁₀	282.05215	[20,
					$-CO]^{+•}$	O ₅	254.05727	21]
					$[(M+H)-CH_3-H_2O]$	C ₁₅ H ₁₀	226.06232	
					$-2CO]^{+•}$	O ₄	197.04445	
					$[(M+H)-C_8H_6O]^+$	C ₁₄ H ₁₀		
						O ₃		
						C ₉ H ₉ O ₅		
Dihydrobaic alein	$C_{15}H_{12}$ O ₅	273.076 17	0.41	40	$[(M+H)-H_2O]^+$	C ₁₅ H ₁₁ O	255.064	[22]
					$[(M+H)-C_2H_2O]^+$	O ₄	65	
					$[(M+H)-C_8H_8]^+$	C ₁₃ H ₁₁ O	231.064	
					$[(M+H)-C_6H_6O_4]^+$	O ₄	82	
						C ₇ H ₅ O ₅	169.012	
						C ₉ H ₇ O	92	

							131.049	
							06	
							271.059	
							69	
							243.059	
							5	
							95	
							179.033	
							4	[20,21]
							74	
							163.038	
							82	
							153.018	
							10	
							253.049	
							56	
							229.049	
							35	
							163.038	
							94	[20,21]
							153.018	
							25	
							145.028	
							40	
							285.075	
							29	
							261.075	
							68	
							179.033	
							5	[20,21]
							89	
							153.018	
							28	
							151.075	
							53	
							245.043	
							93	
							[(M+H)-C ₂ H ₂ O] ⁺	C ₁₃ H ₉ O ₅
							179.034	
							[(M+H)-C ₆ H ₄ O ₂] ⁺	C ₉ H ₇ O ₄
							09	
							[(M+H)-C ₈ H ₆ O ₂] ⁺	C ₇ H ₅ O ₄
							153.018	[21,24]
							[(M+H)-C ₈ H ₆ O ₃] ⁺	C ₇ H ₅ O ₃
							22	
							137.023	
							27	

Nepetin	$C_{16}H_{12}$ O ₇	317.065 57	0.19	20	$[(M+H)-H_2O]^+$	$C_{16}H_{11}O$	299.055	[30,31]
					$[(M+H)-CH_2O]^+$	$C_{15}H_{11}O$	287.055 600	
Naringenin	$C_{15}H_{12}$ O ₅	273.076 29	0.28	20	$[(M+H)-H_2O]^+$	$C_{15}H_{11}$	255.064	[20,2]
					$[(M+H)-C_2H_2O]^+$	O ₄	231.064 87	
Pinocembrin	$C_{15}H_{12}$ O ₄	257.081 32	0.20	20	$[(M+H)-C_8H_8O]^+$	$C_{13}H_{11}$	153.018	[21,2]
					$[(M+H)-C_6H_6O]^+$	O ₄	179.033 101	
Quercetin	$C_{15}H_{10}$ O ₇	303.050 47	0.12	20	$[(M+H)-3C_2H_2O]^+$	$C_7H_5O_4$	147.043	[20,2]
					$[(M+H)-C_8H_8]^+$	$C_9H_7O_4$	93	
Sakuranetin	$C_{16}H_{14}$ O ₅	287.091 32	0.28	20	$[(M+H)-H_2O]$	$C_{15}H_{11}$	239.069	[20,2]
					$[(M+H)-2CO]^+$	O ₃	215.070	
Salvigenin	$C_{18}H_{16}$ O ₆	329.101 44	0.52	40	$[(M+H)-H_2O-2CO]$	$C_{13}H_{11}$	1012	[20,2]
					$[(M+H)-C_8H_6O_3]^+$	O ₅	179.034 51	
						$C_{13}H_9O$	153.018	
						$C_7H_5O_4$	36	
							245.080	
							247.060	
							285.037 87	
							229.049	
							193.049	
							167.033	
							147.044	
							129.02	
							314.077	
							296.067	
							268.072	
							248.00	

Taxifolin	$C_{15}H_{12}$ O ₇	305.065 48	0.30	30	$[(M+H)-H_2O]^+$	C ₁₅ H ₁₁	287.054	[20,2] 12 1]
					O ₆	87		
Scutellarein	$C_{15}H_{10}$ O ₆	287.054 44	0.57	60	$[(M+H)-H_2O-CO]^+$	C ₁₄ H ₁₁	259.060	
					$[(M+H)-H_2O-2CO]$	O ₅	03	
] ⁺	C ₁₃ H ₁₁	231.065	
					$[(M+H)-H_2O-2CO]$	O ₄	213.054	
					$-H_2O]^+$	C ₁₃ H ₉ O	63	
					$[(M+H)-C_8H_8O_3]^+$	C ₇ H ₅ O ₄	153.018	
					³	26		
							269.044	
							16	
					$[(M+H)-H_2O]^+$	C ₁₅ H ₉ O	241.049	
Wogonin	$C_{16}H_{12}$ O ₅	285.075 75	0.49	50	$[(M+H)-H_2O-CO]^+$	⁵	12	[22]
					$[(M+H)-C_8H_6O]^+$	C ₁₄ H ₉ O	169.012	
					$[(M+H)-C_8H_6O-CO]$	O ₄	80	
] ⁺	C ₇ H ₅ O ₅	141.018	
					$[(M+H)-C_8H_6O-CO]$	C ₆ H ₅ O ₄	10	
					$-H_2O]^+$	C ₆ H ₃ O ₃	123.007	
					$[(M+H)-C_7H_4O_5]^+$	C ₈ H ₇ O	71	
							119.049	
							21	
						C ₁₅ H ₁₀	270.051	
Methyl-apigenin	$C_{16}H_{12}$ O ₅	285.076 87	0.37	30	$[(M+H)-CH_3]^{+•}$	O ₅	76	[22]
					$[(M+H)-CH_3-CO]^{+•}$	C ₁₄ H ₁₀	242.057	
						O ₄	01	
						C ₁₅ H ₁₀	270.052	
					$[(M+H)-CH_3]^{+•}$	O ₅	19	
					$[(M+H)-CH_3-CO]^{+•}$	C ₁₄ H ₁₀	242.057	
					$[(M+H)-C_9H_8O]^+$	O ₄	34	
						C ₇ H ₅ O ₄	153.018	
							48	
Methyl-galangin	$C_{16}H_{12}$ O ₅	285.075 63	0.42	30	$[(M+H)-CH_3]^{+•}$	C ₁₅ H ₁₀	270.052	[21]
					$[(M+H)-CH_3-CO]^{+•}$	O ₅	19	
					$[(M+H)-CH_3-CO-H]$	C ₁₄ H ₁₀	242.057	
					$CO]^{+•}$	O ₄	34	
					$[(M+H)-C_9H_8O]^+$	C ₁₃ H ₉ O	213.054	
					³	61		
						C ₇ H ₅ O ₄	153.018	
							30	
Trimethyl-tricetin	$C_{18}H_{16}$ O ₇	345.096 59	0.80	30	$[(M+H)-CH_3]^{+•}$	C ₁₇ H ₁₄	330.073	[20,3] 1]
					$[(M+H)-2CH_3]^+$	O ₇	39	
					$[(M+H)-CH_3-H_2O]^+$	C ₁₆ H ₁₁	315.050	
					•	O ₇	63	

	$[(M+H)-CH_3-H_2O-$	$C_{17}H_{12}$	312.062
	$CO]^{+\bullet}$	O_6	62
	$[(M+H)-C_{11}H_{12}O_3]^+$	$C_{16}H_{12}$	284.067
		O_5	69
		$C_7H_5O_4$	153.018
			17

Tentative identification based on comparison with $[M^+]$ or $[M + H]^+$ ions reported in previous studies and the literature for *Scutellaria* spp. [19,22], *L. origanoides* [20,21,29,30] and *L. alba* [24,32]. Tentative identification based on comparison with molecule fragmentation pattern in mass spectra and on databases [31].

Table 4. Amounts (mg/g) of flavonoids in extracts prepared in the study.

Name	<i>Scutellaria</i>		<i>L. alba</i>		<i>L. origanoides</i>			
	SiSE2	SviSE	LacSE	LaiSE	LopSE2	LocSE1	LocSE2	LotSE
Flavonoid glycosides								
Apigenin-7-glucoside	<LOD	-	<LOD	<LOD	<LOD	0.04 ± 0.01	<LOD	0.62 ± 0.2
Apigenin-7-glucuronide ^a	-	-	1.5 ± 0.09	2.3 ± 0.19	14 ± 1.00	-	27 ± 1.40	-
Baicalin	15.9 ± 0.02	16 ± 0.02	-	-	-	-	-	-
Chrysoeriol-7-glucuronide	-	-	3.8 ± 0.05	3.5 ± 0.01	-	-	-	-
Chrysoeriol-7-diglucuronide	-	-	4.9 ± 0.07	2.5 ± 0.03	-	-	-	-
Dihydrobaicalein-glucuronide ^a	23 ± 0.006	<LOD	-	-	-	-	-	-
Eriodictyol-7-glucoside	-	-	-	-	80 ± 2.00	0.36 ± 0.03	89 ± 1.30	3.2 ± 0.3
Eriodictyol-rhamnoside	-	-	-	-	-	0.13 ± 0.01	-	0.32 ± 0.03
Galangin-glucoside	-	-	-	-	-	<LOD	-	-
Luteolin-7-glucoside	-	-	0.6 ± 0.11	0.68 ± 0.04	49 ± 1.00	0.25 ± 0.02	35 ± 0.10	5.01 ± 0.3
Luteolin-7-glucuronide	-	-	0.8 ± 0.19	1.1 ± 0.33	-	-	-	-
Luteolin-rutinoside	-	-	-	-	-	0.02 ± 0.01	-	0.10 ± 0.01
Quercetin-3-glucoside	-	-	-	-	<LOD	1.5 ± 0.3	<LOD	6.2 ± 0.8
Scutellarin	11.4 ± 0.03	11.4 ± 0.03	-	-	-	-	-	-
Taxifolin-glucoside	-	-	-	-	-	<LOD	-	<LOD
Tricin-glucuronide	-	-	3.7 ± 0.12	2.8 ± 0.03	-	-	-	-
Tricin-7-diglucuronoside	-	-	5.5 ± 0.13	3.8 ± 0.04	-	-	-	-
Wogonoside	4.7 ± 0.03	4.7 ± 0.03	-	-	-	-	-	-
Phloridzin	-	-	-	-	-	0.01 ± 0.01	-	0.05 ± 0.04
Flavonoid aglycones								
Acacetin	-	-	<LOD	<LOD	-	-	-	-
Apigenin	-	-	0.34 ± 0.06	1.2 ± 0.39	-	0.13 ± 0.01	-	-
Baicalein	10.1 ± 0.04	10 ± 0.04	-	-	-	-	-	-
Chrysoeriol	-	-	-	-	-	0.70 ± 0.04	-	-
Cirsimarin	-	-	0.31 ± 0.02	0.40 ± 0.14	-	0.9 ± 0.04	4.3 ± 0.10	0.38 ± 0.01
Baicalein	10.1 ± 0.04	10 ± 0.04	-	-	-	-	-	-
Chrysoeriol	-	-	-	-	-	0.70 ± 0.04	-	2.3 ± 0.1
Cirsimarin	-	-	0.31 ± 0.02	0.40 ± 0.14	-	0.9 ± 0.04	-	2.9 ± 0.2
Dihydrobaicalein ^c	4.13 ± 0.007	<LOD	-	-	-	-	-	-



Eriodictyol	-	-	-	-	89 ± 1.00	4.5 ± 0.03
Galangin	-	-	-	-	50 ± 2.00	<LOD
Hesperetin	-	-	-	-	-	0.17 ± 0.01
Luteolin	-	-	<LOD	<LOD	7.3 ± 0.20	1.12 ± 0.05
Naringenin	-	-	<LOD	<LOD	6.0 ± 0.20	1.38 ± 0.05
Nepetin	-	-	<LOD	<LOD	-	-
Pinocembrin	-	-	-	-	71 ± 2.00	0.03 ± 0.01
Quercetin	-	-	-	-	<LOD	1.5 ± 0.1
Sakuranetin	-	-	-	-	<LOD	0.32 ± 0.02
Salvigenin	-	-	<LOD	<LOD	-	-
Scutellarein	0.2 ± 0.2	$0.2 \pm$ 0.20	-	-	-	-
Taxifolin	-	-	-	-	4.8 ± 0.10	0.47 ± 0.02
Wogonin	$15.4 \pm$ 0.03	$15 \pm$ 0.03	-	-	-	-
Methylated flavonoids						
Methylapigenin	-	-	-	-	-	0.03 ± 0.01
Methylgalangin	-	-	-	-	<LOD	<LOD
Trimethyltricetin	-	-	-	-	-	0.03 ± 0.01

All extracts were prepared using the UAE technique (Table 1). Extracts from *S. incarnata* (SiSE2), *S. ventenatti* + *S. incarnata* (SviSE), *L. alba* carvone (LacSE) and citral (LaiSE) chemotypes; and *L. organoides* phellandrene (LopSE2), carvacrol (LocSE1 and LocSE2) and thymol (LotSE) chemotypes. a Quantification in baicalin; b quantification in wogonoside; c quantification in baicalein equivalents; d quantification in 1,3-dicaffeoylquinic acid equivalents. LOD: limit of detection. Wogonoside (LOD = 0.05 mg/g), eriodictyol-7-glucoside (LOD = 0.04 mg/g), baicalin (LOD = 0.80 mg/g), and scopoletin (LOD = 0.05 mg/g).

Extracts from *Scutellaria* (UAE, 60 min at 50 °C) had higher concentrations of flavonoid glycosides than aglycones. Nine flavonoids were detected in *S. incarnata* (SiES2), with glycosides accounting for 64.7% (55-85 mg/g) of the total content. The predominant flavonoids were dihydrobaicalein-glucuronide, scutellarin, baicalin, baicalein, and wogonin. The flavonoid content of the *S. ventenatti* + *S. incarnata* (SviSE) extract was similar to that of SiES2, except for the absence of dihydrobaicalein-glucuronide and dihydrobaicalein. Flavonoid glycosides accounted for 55% (32/58 mg/g) of the SviSE content.

L. alba extracts (UAE, 60 min at 50 °C) had high flavonoid glycosides content, exceeding levels reported in extracts of the same species cultivated in Brazil [32], which may be attributed to variations in extraction methodology and cultivation practice of the plant. In the LaiSE (citral chemotype) extract were identified eight flavonoid glycosides accounting for 90.7% (16.6/18.3 mg/g) of total content. Tricin-7-diglucuronide, chrysoeriol-7-diglucuronide, chrysoeriol-7-glucuronide, tricin-glucuronide, and apigenin-7-glucuronide were predominant. Seven flavonoids aglycones were also identified, five from which were below detection limits. The LacSE (carvonal chemotype) extract exhibited a comparable profile, yet with higher amounts of flavonoid glycosides (97.1%, 20.7 / 21.3 mg/g).

L. organoides extracts had higher flavonoid aglycone content than the other test extracts. Notable differences were observed in extracts from the carvacrol chemotype. LocSE1 (UAE, 23 min at 47 °C) contained twenty-four flavonoids, 82.3% (11.2/13.6 mg/g) of which were aglycones. Eriodictyol, naringenin, luteolin, quercetin, and cirsimarinin were predominant. The LocSE2 extract (UAE, 60 min at 50 °C) contained twelve flavonoids in higher amounts (259 mg/g vs. 13.6 mg/g), with aglycones accounting for 41.7%. The predominant flavonoids were eriodictyol, eriodictyol-7-glucoside, and luteolin-7-glucoside. The thymol chemotype LotSE (UAE, 23 min at 47 °C) extract contained twenty-three flavonoids. Aglycones accounted for 73.1% (42/57.4 mg/g), with eriodictyol, quercetin, and naringenin as the predominant. The phellandrene chemotype LopSE2 (UAE, 60 min at 50 °C) extract contained fourteen flavonoids, with aglycones accounting for 61.5% (228/371 mg/g) with eriodictyol, pinocembrin, and galangin as the predominant.

2.4. Relationship Between Anti-DENV Effect and the Flavonoid Content

Fourteen extracts listed in Table 1 were included in the analysis. The chemical compositions of six extracts that were analyzed in previous studies are shown in Table S1. The relationship between antiviral effect and the flavonoid content was investigated to test the hypothesis that extracts exhibiting anti-DENV effect (strong or weak) possess distinct chemical profiles compared to inactive extracts. Table 5 compares flavonoid classes identified in the fourteen extracts.

Table 5. Antiviral effect and relative concentrations of flavonoid classes of the extracts.

Extract	Antiviral effect	Total (mg/g)	Glycoside (%)				Aglcone (%)			Methylated (%)
			A	B	C	D	A	B	C	
ScSE	Strong	277.86	83.4	4.1	0	0.56	10.3	0	0	0
SiSE1	Strong	492.98	86.1	2.5	0	0	5.0	0	0	0
SviSE	Weak	57.92	55.5	0	0	0	44.5	0	0	0
LacSE	Weak	21.37	97.0	0	0	0	3.0	0	0	0
LaiSE	Weak	18.34	90.7	0	0	0	9.3	0	0	0
SiSE2	Inactive	84.92	64.8	0	0	0	35.2	0	0	0
LopSE1	Inactive	27.58	24.7	15	37	0.9	3.9	10.1	8.0	0.4
LopSE2	Inactive	371.10	17	21.6	0	0	2.0	44.7	14.8	0
LocSE1	Inactive	13.59	2.3	3.6	11.0	0.07	21.0	47.1	14.5	0.4
LocSE2	Inactive	259.00	23.9	34.4	0	0	1.7	38.2	1.8	0
LotSE	Inactive	57.44	10	6.1	10.8	0.1	15.1	41.4	16.2	0.2
LopSFE	Inactive	62.96	0	0	0	0	0.2	81.4	11.8	6.5
LocSFE	Inactive	19.85	0	0	0	0	21.4	70.7	6.0	1.9
LotSFE	Inactive	25.90	0	0	0	0	25.8	68.0	0.8	5.4

The total flavonoid content was found to account for 100% of the compounds identified in all extracts, except ScSE (89.5%) and SiSE1 (93.5%). A: Flavone. B: Flavanone. C: Flavanol + Flavanonol. D: Chalcone. Data are derived from both Table 3 and Table S1.

Extracts with the strongest anti-DENV effects (ScSE and SiSE1) contained high amounts of flavonoids (278 mg/g and 493 mg/g, respectively). Of these flavonoids, 83.4% and 86.1%, respectively, corresponded to flavone glycosides, with baicalin, dihydrobaicalein-glucuronide, and scutellarin being the predominant flavones. ScSE and SiSE1 also had small amounts of flavone aglycones (10.3% and 5%, respectively) and non-flavonoid compounds (6.4% and 10.5%), including verbascoside and umbelliferone-hexoside-pentoside (Table S1). In contrast, extracts with weak anti-DENV effects (SviSE, LacSE, and LaiSE) had significantly lower amounts of flavonoid (from 18.3 mg/g to 57.9 mg/g), though most of these were flavone glycosides (56.5%, 97%, and 90.7%, respectively). Among the extracts with anti-DENV effect, SviSE contained a significantly higher concentration (44.5%) of flavonoid aglycones, all of them belonging to the flavone class. The *S. incarnata* SiSE2 extract, lacking anti-DENV effect, had a chemical profile comparable to SviSE, except for the lack of dihydrobaicalein.

Extracts from *L. organoides* lacking anti-DENV effect had the lowest concentrations of flavone glycosides (0 to 23.9%) but the highest of aglycones (61.5% to 98.1%), especially flavanone and flavanol + flavanonol, which were absent in extracts showing anti-DENV effects. Furthermore, UAE extracts (LopSE1, LopSe2, LocSE1, and LocSE) exhibited higher levels (17% to 34.4% vs. 0 to 4.6%) of flavonoid glycosides distinct to flavones, while SFE extracts lacked of flavonoid glycosides and contained small amounts of methylated flavonoids. The UAE-LopSE1 extract (phellandrene chemotype) had higher levels of flavonoid glycosides (77.4%) than aglycones (22.2%) compared to other *L. organoides* extracts.

A Kohonen's self-organized map algorithm, using percentages of flavonoid classes as input, grouped the fourteen extracts into two clusters (Figure 3A). Cluster 1 included five anti-DENV active extracts (*Scutellaria* and *L. alba*) along with the inactive *S. incarnata* extract (SiSE2). These extracts shared the highest flavone glycosides content and lowest flavonoid aglycones. Cluster 2 grouped seven inactive *L. organoides* extracts marked by elevated flavonoid aglycones levels. The LopSE1 extract from *L. organoides* was not included in cluster 2, as would have been expected, due to its distinct chemical profile. Figure 3B and 3C show that CPE values for DENV-1 and DENV-2 were

significantly lower in cluster 1 compared to cluster 2 (Wilcoxon test, $p < 0.01$). This suggests a plausible relationship between the anti-DENV activity and a flavonoid profile characterized by a higher content of flavonoid glycosides, especially flavones, relative to flavonoid aglycones.

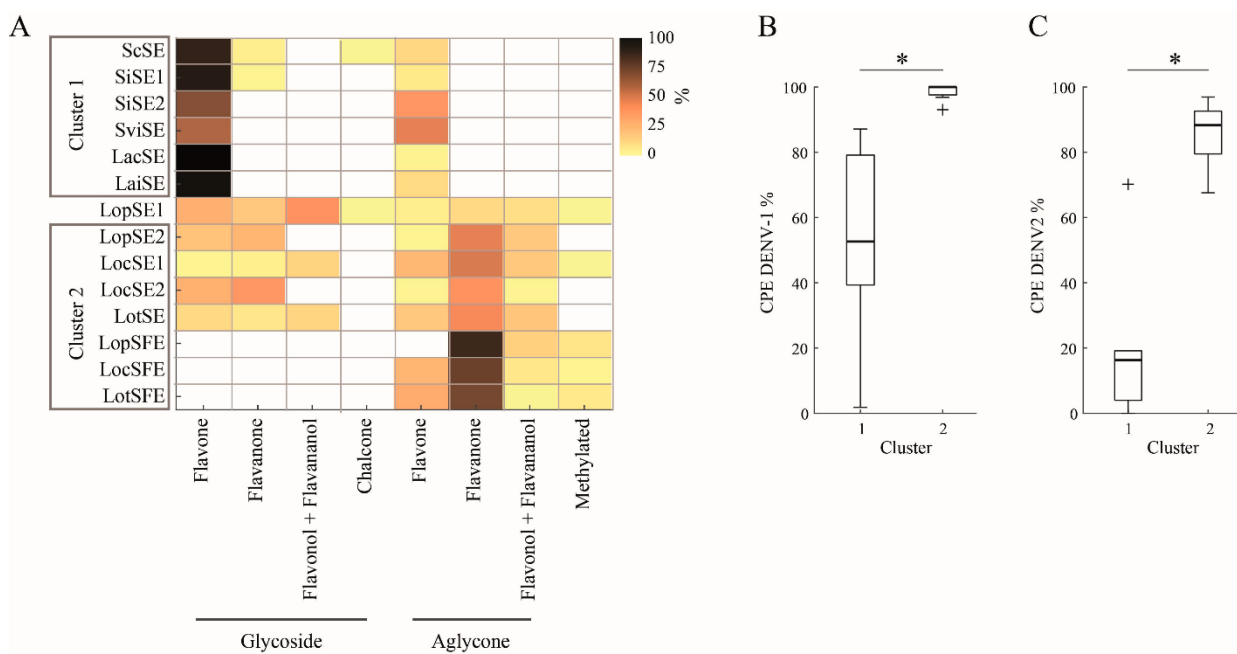


Figure 3. Relationship between flavonoid profiles and anti-DENV effects of the extracts. **A.** Heatmap showing the content of flavonoid classes and revealing two clusters obtained by an unsupervised self-organizing map. **B** and **C**. Comparison of antiviral activity (CPE, cytopathic effect percentage) of clusters against DENV-1 (*) Wilcoxon test $Z = -2.969$; $p = 0.003$) and DENV-2 (*) Wilcoxon test $Z = -2.785$; $p = 0.0053$).

2.5. Molecular Interactions Between Flavonoids and DENV and Vero Cell Proteins

DENV infection of Vero cells is initiated by the interaction between its envelope (E) protein and specific cell surface receptors, including Axl receptor tyrosine kinase [34]. The virus enters cells via a non-classical endocytic pathway mediated by the clathrin and dynamin proteins [35–37]. To explore the role of flavonoids in the anti-DENV effect, an AutoDock Vina software was used to dock forty-six flavonoids found in fourteen extracts to the DENV-E, Gas6-Axl complex, clathrin, and dynamin. Binding energy values of ≤ -7.55 kcal/mol indicate binding affinity between ligand and target. Figure 4 shows the relative concentrations of flavonoids in the extracts and their binding affinities to proteins. As expected, the analysis revealed varied binding affinities to targets. Generally, glycosides exhibited higher binding affinities (energy ranging from -10.22 to -8.01 kcal/mol) compared to aglycones (-8.23 to -7.90 kcal/mol), a difference that can be influenced by the presence of sugar. Most flavonoid glycosides exhibiting the lowest binding energies were the most abundant in extracts with anti-DENV effect.

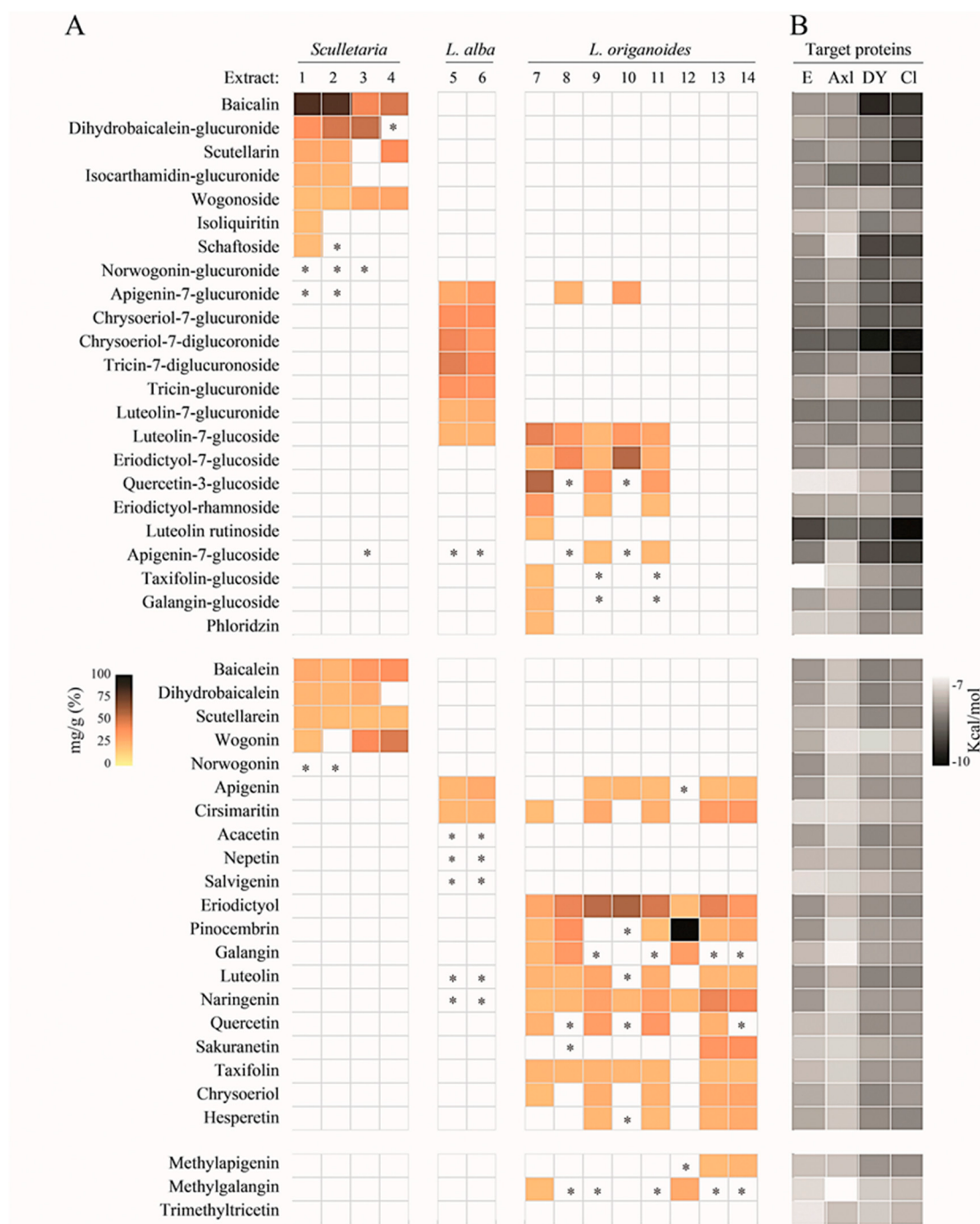


Figure 4. Heatmaps showing the abundance of each flavonoid and its binding affinity for target proteins. **A.** Relative concentration (mg/g) of flavonoid in the extract (Table 4): 1, ScSE; 2, SiSE1; 3, SiSE2; 4, SviSE; 5, LacSE; 6, LaiSE; 7, LopSE1; 8, LopSE2; 9, LocSE1; 10, LocSE2; 11, LotSE; 11, LopSFE; 12, LocSFE; and 13, LotsSFE. **Scutellaria** (1,2 and 4) and **L. alba** (6 and 7) exhibited anti-DENV effect, while the others extracts were inactive. * Low detection limit. **B.** Binding affinities (kcal/mol) of flavonoids for target proteins: E, DENV-2 E envelope; GX, Gas6-Axl receptor; Cl clathrin N-terminal domain (2XZG); DY, dynamin GTPase domain.

The DENV-E protein structure consists of three domains [33], DI and DII domains form the DI/DII hinge region containing a conserved fusion loop. Conformational changes in this region lead to the fusion of the viral and cell endosomal membranes [37]. Nineteen glycosides (-9.16 to -7.72 kcal/mol) and fourteen aglycones (-8.06 to -7.55 kcal/mol) were predicted to bind to E. As for flavonoids found in extracts with antiviral effect, all flavone glycosides exhibited affinity (-8.78 to -7.72 kcal/mol) for E, except schaftoside. The lowest binding energies were exhibited by chrysoeriol-7-diglucuronide, chrysoeriol-7-glucuronide, luteolin-7-glucuronide, apigenin-7-glucuronide, and

tricin-7-diglucuronide, all of which are predominant in *L. alba* extracts. All flavonoid aglycones, except cirsimarinin, exhibited affinity for E; the predominant baicalin, dihydrobaicalin, and apigenin showed the lowest energies (-7.96 to -7.84 kcal/mol). As for flavonoids present in extracts lacking antiviral effect (*L. organoides*), 50% glycosides non-flavones (-8.08 to -7.73 kcal/mol) and 50% aglycones (-8.05 to -7.73 kcal/mol) exhibited affinity for E. Eriodictiol-7-glucoside, eriodictiol, and pinocembrin had the lowest binding energies. Flavonoids formed hydrogen bonds with amino acid residues at three consensus binding sites (Figure 5). Most glycosides were accommodated within the DII domain closer to the dimer interface (A/B), with the remaining glycosides located within the interface DIII/DI domains closer to the fusion loop. Most aglycones were accommodated within the detergent β -octyl glucoside (β OG) site in the hinge region, with the remaining aglycones located within the DII (A/B) interface.

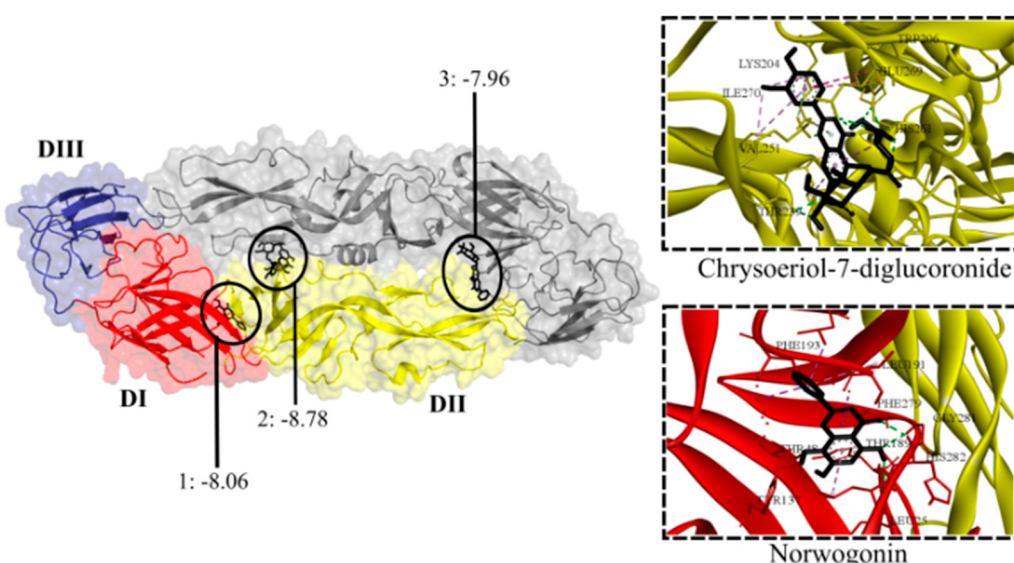


Figure 5. Contact preferences at the DENV-E protein (PDB ID: 1OAN) of representative flavonoids. Norwogonin (1) within the DI/DII hinge region around the β OG pocket; chrysoeriol-7-diglucuronide (2) within the interface of DII domains; and baicalin (3) within the DIII/DI interface. Binding free energies (kcal/mol) are shown.

DENV can bind to the Axl receptor via the Gas6 protein, which facilitates virus entry by bridging the viral envelope's phosphatidylserine to Axl [34]. Gas6 has two domains (Lg1 and Lg2) that interact with Axl domains (Ig1 and Ig2). Sixteen flavonoid glycosides were predicted to bind to Gas6 (-8.66 to -7.56 kcal/mol), whereas no aglycones (-7.52 to -6.83 kcal/mol) exhibited binding affinity. All flavone glycosides found in anti-DENV extracts exhibited affinity (-8.69 to -7.56 kcal/mol) for Gas6, except for schaftoside. The lowest binding energies were exhibited by chrysoeriol-7-diglucuronide, tricin-7-diglucuronide, luteolin-7-glucuronide, and luteolin-7-glucoside. In contrast, only two (eriodictiol-7-glucoside and eriodictiol-rhamnoside) from six glycosides non-flavones found in inactive extracts were predicted to bind to Gas6 (-7.77 kcal/mol and -7.76 kcal/mol, respectively). Flavonoid glycosides formed hydrogen bonds with amino acid residues at five consensus binding sites (Figure 6). Most flavonoids were located within the interface of Gas6-Lg2/Lg1 domains in which each of the monomers. The remaining flavonoids were accommodated within the Gas6-Lg1 domain, and the interface of the Gas6-Lg1/Axl domains within each of the monomers.

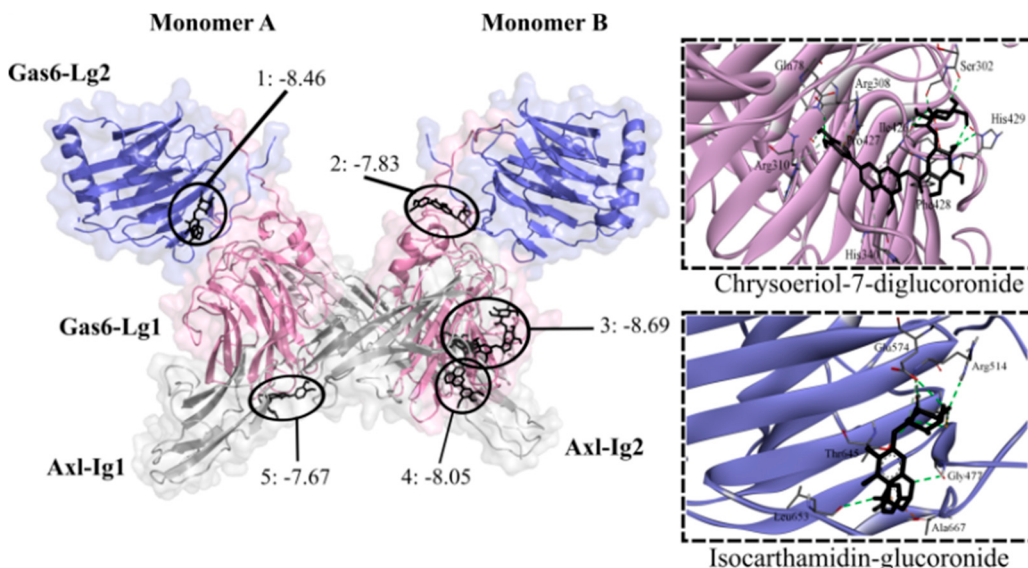


Figure 6. Contact preferences at the Gas6-Axl complex (PDB ID: 2C5D) of representative flavonoids. Isocarthamidin-glucuronide (1) and chrysoeriol-7-glucuronide (2) within Gas6-Lg2/Lg1 domains; chrysoeriol-7-diglucuronide (3) within Gas6-Lg1 domain; tricin-7-diglucuronoside (4) within Gas6-Lg1/Axl-Ig2 domains; and eriodyctiol-rhamnoside (5) within Gas6-Lg1/Axl-Ig1 domains. Binding free energies (kcal/mol) are shown.

Dynamin possess a GTPase domain that binds to and hydrolyzes guanosine-5'-triphosphate (GTP), causing a conformational change crucial for its function in DENV and cell membranes fusion [39]. Small molecules targeting GTPase can interfere with virus internalization [39]. All twenty-three flavonoid glycosides (-9.96 to -7.68 kcal/mol), except quercetin-3-glucoside, were predicted to bind to GTPase. The glycosides with the lowest binding energies were chrysoeriol-7-diglucuronide, baicalin, isoliquiritin, apigenin-7-glucoside, and chrysoeriol-7-glucuronide. These flavonoids are found in anti-DENV extracts but not in inactive *L. organoides* extracts. Seventeen aglycones exhibited binding affinity for GTPase (-8.26 to -7.73 kcal/mol). Baicalein, dihydrobaicalein, luteolin, and scutellarein had the lowest binding energies. The flavonoids formed hydrogen bonds with amino acid residues of five consensus binding sites (Figure 7). Most glycosides were accommodated at the G4 loop extending to the switch1 loop (G4-switch1 loops), while others were accommodated within the P-loop and a few at the switch1 or switch2, closer to the P-loop (switch1-P-loops and switch2-P-loops). Most aglycones were accommodated at the switch2-P-loops and G4-switch1-loops.

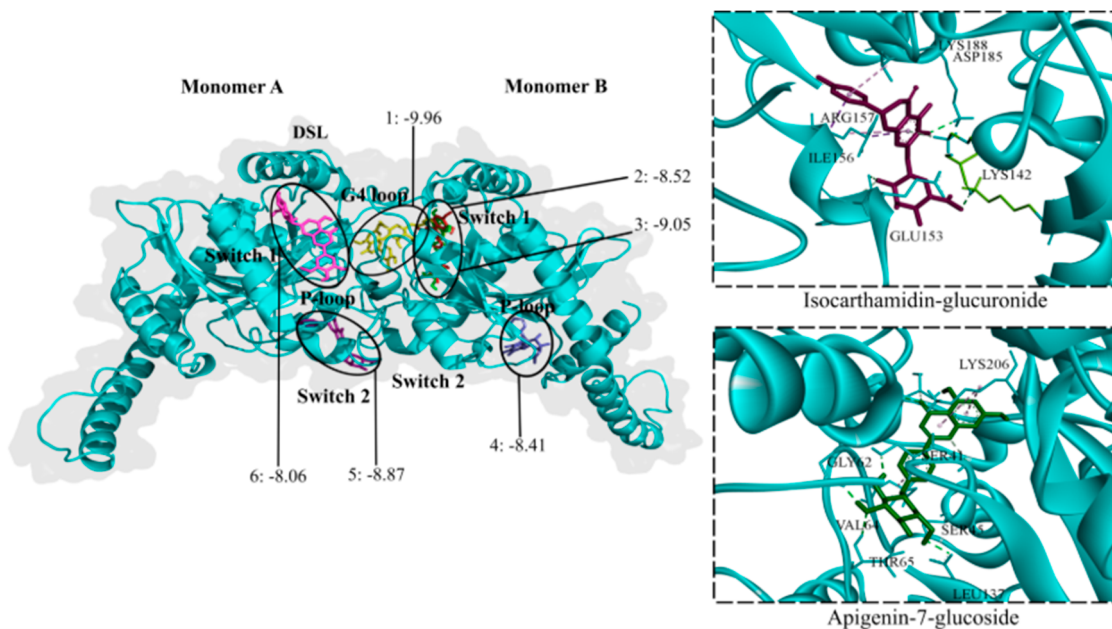


Figure 7. Contact preferences at the GTPase domain (PDB ID: 2X2E) of representative flavonoids. Chrysoeriol-7-diglucuronide (1) within the G4-switch1-loops; apigenin-7-glucoside (2) closer to the switch1-loop; luteolin-7-glucuronide (3) within switch1-P-loops; dihydrobaicalein-glucuronide (4) closer to the P-loop; isocarthamidin-glucuronide (5) within the switch2-P-loops; and tricin-glucuronide (6) within the switch1-loop. Binding free energies (kcal/mol) are shown.

Clathrin is a transport protein whose N-terminal domain (CTD) has various peptide-binding sites, including the PWDLW motif (W-box) [38]. CTD has been proposed as a target for antiviral agents that hinder viral entry into the cell [40]. All of the flavonoid glycosides were predicted (-10.01 to -8.08 kcal/mol) to bind to CTD, except for quercetin-3-glucoside. The lowest binding energies were observed for chrysoeriol-7-diglucuronide, triicin-7-diglucuronide, apigenin-7-glucoside, baicalin, and scutellarin. All flavonoid aglycones except wogonin exhibited binding affinity for CTD (-8.22 to -7.75 kcal/mol). Luteolin, eriodictyol, hesperetin, nepetin, and baicalein had the lowest binding energies. Both glycosides and aglycones formed hydrogen bonds with amino acid residues in the W-box motif (Figure 8).

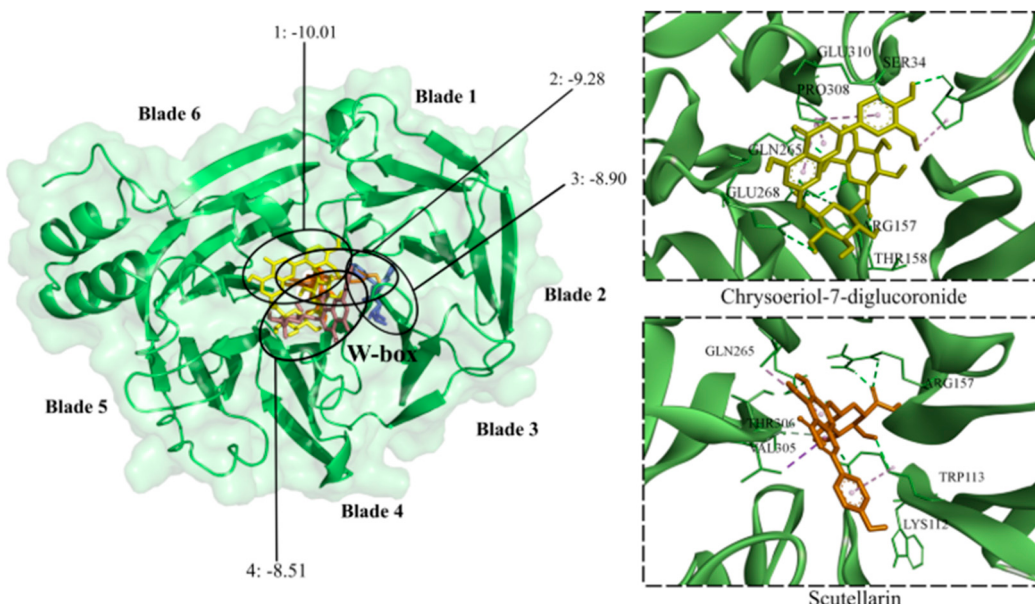


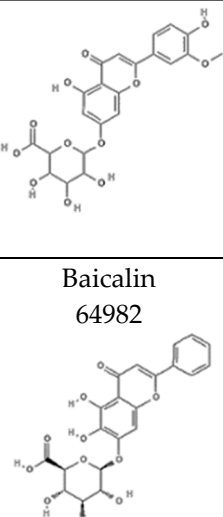
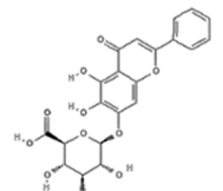
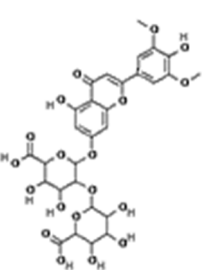
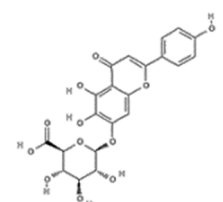
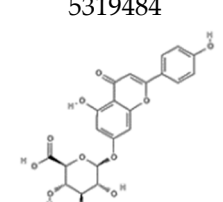
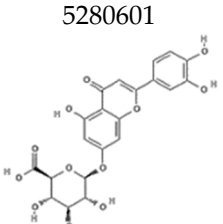
Figure 8. Contact preferences at the CTD-clathrin domain (PDB ID: 2XZG) of representative flavonoids. Chrysoeriol-7-diglucuronide (1), scutellarin (2), dihydrobaicalein-glucuronide (3), and wogonoside (4) within the W-box motif. Binding free energies (kcal/mol) are shown.

Molecular docking results for the predominant flavonoids of extracts from *Scutellaria* and *L. alba* are showed in Table 6. Results for the other flavonoids are shown in Table S1 and Table S2.

Table 6. Binding mode predicted for the predominant flavonoids in extracts from *Scutellaria* species and *L. alba* to targets. Protein (PDB ID): Cl, clathrin N-terminal domain (2XZG); DENV-2 E, envelope (1OAN); DY, dynamin GTPase domain (2X2E); GX: Gas6-Axl receptor (2C5D).

Name/PubChem CID/formula	Target: site	Amino acids interacting through hydrogen bonds	kcal/mol
	Cl: W-box	Ser34, Thr158, Gln265, Glu268, Arg157.	-10.01 ± 0.27
Chrysoeriol-7-diglucoronide 44258206	DY: G4-switch1	Ser41, Gly60, Lys113, Ala177, Asp180, Leu181, Lys206, Thr214, Asn236, Gln239.	-9.96 ± 0.44
	E: DII (A/B)	Trp206, Thr239, His261, Thr265, Glu269, Ile270.	-8.78 ± 0.37



	GX: Gas6-Lg1	Gln78, Ser304, Gly307, Arg308, Leu309, Gln341, Ile426, Phe428, His429.	-8.69 ± 0.18
Baicalin 64982 	DY: G4-switch1	Ser41, Gly60, Ser61, Ala177, Asp180, Lys206, Thr214.	-9.67 ± 0.17
	Cl: W-box	Glu33, Lys112, Asn155, Arg157, The158, Met264, Gln265, Thr306	-9.33 ± 0.49
	GX: Gas6-Lg1/Lg2	Met644, Thr645, Asp654, Leu655, Ala667.	-7.96 ± 0.18
	E: DII/DI	Arg2, Glu44, Ile46, Asp98.	-7.96 ± 0.22
Tricin-7-diglucuronoside 131752191 	Cl: W-box	Lys112, Arg157, Ser200, Phe201, Met264, Gln265, Ile266, Glu268, Thr306, Gly314.	-9.45 ± 0.17
	E: DII (A/B)	Leu65, Asp203, Lys204, Ala205, Val252, His261, Glu269.	-8.29 ± 0.21
	DY: P-loop	Gln33, Arg67, Arg107, Gln117, Asn126, Asp130, Leu131, Lys166.	-7.88 ± 0.14
	GX: Gas6-Lg1/Axl-Ig2	Gln78, Ser302, Gly303, Arg308, Leu309, Gln341, Ile426, Phe428, His429.	-8.05 ± 0.20
Scutellarin 185617 	Cl: W-box	Trp111, Lys112, Trp113, Arg157, Thr158, Met264, Gln265, Thr306.	-9.28 ± 0.39
	DY: G4-switch1	Ser61, Asp180, Leu181, Lys206, Thr214.	-8.31 ± 0.16
	E: DII (A/B)	Asp203, Lys204, Ala205, Thr262, Leu264, Thr265, Glu269.	-8.13 ± 0.32
	GX: Gas6-Lg1/Lg2	Glu331, Asn438, Arg476, Gly477, Asp654, Glu657, Ala667.	-7.80 ± 0.17
Apigenin-7-glucoronide 5319484 	Cl: W-box	Lys112, Thr158, Gln265, Thr306	-9.17 ± 0.27
	DY: G4-switch1	Ser41, Ala42, Gly43, Lys44, Ser45, Ser46, Gly60, Val64, Thr65, Gln239.	-8.70 ± 0.16
	E: DII (A/B)	Asp203, Lys204, Leu264, Thr262, Glu269.	-8.22 ± 0.17
	GX: Gas6-Lg1/Lg2	Phe328, Asn438, Arg476, Gly477, Asp654, Glu657, Ala667, His668.	-7.82 ± 0.17
Luteolin-7-glucuronide 5280601 	Cl: W-box	Glu33, Ser70, The109, Lys112, Ile153	-9.10 ± 0.26
	DY: G4-switch1	Ser41, Ala42, Gly43, Lys44, Ser46, Arg59, Gly60, Val64, Thr65, Lys206, Leu207, Asn236.	-8.52 ± 0.18
	E: DII (A/B)	Lys204, Ala205, Thr265, Ala267, Glu269	-8.41 ± 0.15
	GX: Gas6-Lg2	Gly477, Arg514, Asp654, Ala667.	-8.25 ± 0.21

Tricin-glucuronide 101939793	Cl: W-box GX: Gas6-Lg1/Lg2 E: DII (A/B) DY: P-loop	Lys112, Arg157, Ser200, Phe201, Met264, Gln265, Ile266, Glu268, Thr306, Gly314. Gln78, Ser302, Gly303, Arg308, Leu309, Gln341, Ile426, Phe428, His429. Leu65, Asp203, Lys204, Ala205, Val252, His261, Glu269, Trp206. Gln117, Asn126, Asp130, Leu131, Gln33, Arg67, Arg107, Lys166.	-9.45 ± 0.17 -8.05 ± 0.20 -8.29 ± 0.20 -7.88 ± 0.14
Dihydrobaicalein-glucuronide 14135324	Cl: W-box DY: P-loop GX: Gas6-Lg2 E: DI/DII	Ser28, Ser70, Thr109, Gln152, Ile153. Gln17, Asn26, Asn121. Gln78, Arg308. Gly102, Asn103, His149, Gly152, Asn153, Asp154, Thr155.	-8.90 ± 0.27 -8.41 ± 0.20 -7.99 ± 0.20 -7.72 ± 0.34
Isocarthamidin-glucuronide 101274424	DY: switch2-P Cl: W-box GX: Gas6-Lg1/Lg2 E: DI/DII	Lys142, Glu153, Lys188. Trp113, Arg157, Met264, Gln265, Glu268, Thr30. Arg476, Gly477, Ser478, Arg514, Thr645. Asn103, Val151, Asp154, Thr155, His244, Lys246.	-8.87 ± 0.26 -8.78 ± 0.35 -8.46 ± 0.18 -7.97 ± 0.24
Chrysoeriol-7-glucuronide 14630700	DY: G4-switch1 Cl: W-box E: DII (A/B) GX: Gas6-Lg1/Lg2	Ser41, Val64, Thr65, Ser179, Asp180, Lys206, Thr214, Asp215. Met32, Asn155, Gln265, Thr306, Glu301. Lys204, Trp206, Thr262, Leu264, Thr265, Glu269. Lys290, Arg467, Ser663, Asp664.	-8.85 ± 0.43 -8.85 ± 0.27 -8.37 ± 0.16 -7.83 ± 0.16
Luteolin-7-glucoside 5280637	Cl: W-box GX: Gas6-Lg2 DY: G4-switch1 E: DII (A/B)	Ser70, Thr109, Lys112, Ile153. Ser478, Arg514, Cys643, Asp654, His668. Gly60, Ala177, Lys206, Leu209, Asp211, Asp236. Lys204, Ala205, Thr262, Thr265.	-8.54 ± 0.26 -8.18 ± 0.19 -8.00 ± 0.24 -7.98 ± 0.17
Wogonoside 3084961	Cl: W-box E: DII (A/B) DY: G4-switch1 GX: Gas6-Lg1/Lg2	Arg157, Thr158, Ala160, Gln162, Phe201, Gln203, Glu268. Trp206, Gln256, Gly258, Leu264, Thr265, Glu269. Arg67, His85, Arg107, Asn121. Gln78, Leu309, Arg310, Gln341.	-8.51 ± 0.20 -7.94 ± 0.24 -7.69 ± 0.19 -7.69 ± 0.12

Baicalein 5281605	DY: switch2-P Cl: W-box E: βOG pocket	Thr141, Glu153, Arg157, Asp185. Asn155, Arg157, Val262, Met264, Gln265, Thr306. His27, Thr48, Gly281, His282.	-8.26 ± 0.36 -8.08 ± 0.47 -7.92 ± 0.76
Dihydrobaicalein 9816931	DY: switch2-P Cl: W-box E: βOG pocket	Thr141, Glu153, Arg157, Asp185. Ser70, Lys83, Trp111. Leu25, His27, Thr48, Gly281, His282.	-8.25 ± 0.40 7.97 ± 0.45 -7.84 ± 0.80
Wogonin 5281703	E: βOG pocket	Thr48, Tyr137, Gly281, His281.	-7.66 ± 0.80

Both apigenin-7-glucuronide and luteolin-7-glucoside were found in extracts from *L. origanoides*.

3. Discussion

This study analyzed fourteen plant extracts from *Scutellaria* and *Lippia* species cultivated in Colombia that were prepared under varying experimental conditions. Chemical analysis indicated that flavonoids constituted over 100% of their content. UAE-extracts exhibited significant differences in their chemical profiles. Retention of flavonoid glycosides was greater with shorter extraction times (5 or 23 minutes) than with longer times (15 or 60 minutes). This trend was evident in comparisons between SiSE1 vs SiSE2 as well as LopSE1 vs LopSE2 extracts. The reduction in flavonoid glycosides by prolonged extraction is likely due to excessive sonication that facilitate thermal, oxidative, and mechanical degradation, which particularly affect thermolabile glycosides and phenolic compounds [41,42]. Time-dependent variation in the extraction process critically influences the chemical profiles, and ultimately, the abundance of bioactive compounds [41]. SFE is a highly efficient technique for extracting aglycone-rich fractions with limited recovery of water-soluble or glycosylated phytochemicals [43]. The SFE extracts of *L. origanoides* contained high levels of flavonoid aglycones and lacked glycosides, reflecting the principle that nonpolar CO₂ extraction selectively enriches lipophilic compounds while excluding polar glycosides [43]. Chemical profiles of the extracts analyzed in this study differ from those reported for extracts of the same plant [19,28–30,32]. These variations can be explained by differences in growth stage and plant part, cultivation practice, and preparation technique.

The potential of crude plant extracts to inhibit DENV replication *in vitro* has been widely documented [5–7]. However, relationships between their chemical composition and anti-DENV effect remain to be elucidated. This study integrates UHPLC/ESI-Q-Orbitrap-MS data with CPE-DENV reduction data showing that higher contents of flavonoid glycosides, predominantly flavones, correlate with greater inhibitory effect on DENV replication in Vero cells. Moreover, increased aglycones contain is associated with lack of antiviral action, as evidenced by the extracts from *L. origanoides*. The distinction between *S. inamata* extracts is notable: SiSE1 showed strong antiviral effect, whereas SiSE2 had none. SiSE2 contained lower flavonoid glycoside content (64.8% vs. 88.6%)

and sevenfold higher aglycones (35.2% vs. 5.0%). In a previous study, we compared the anti-DENV effects of LopSE1 (77% glycosides) and LopSFE (no glycosides) extracts from *L. origanoids*. After treatment during DENV-1 adsorption on human hepatic cells, the level of viral NS1 protein was significantly reduced by LopSE1, but not by LopSFE. The flavonoid content is a determining factor in the antiviral action of plant extracts on virus others than DENV [8,44]. Glycosylation may enhance flavonoid interactions with virus particles or cell surface receptors by increasing polarity or specific binding conformations relative to aglycones [44]. A study revealed that baicalin exhibited higher anti-DENV activity than baicalein in virus-infected cells [45]. Other study revealed that myricetin and its glycosides exhibited higher antiviral activity against HIV-1 virus compared to their aglycone counterparts [46].

While mechanisms underlying plant extract antiviral activity are yet to be fully elucidated, flavonoids are widely accepted as primary agents [10,11]. Certain flavonoids can interfere with viral adsorption to host cells through the attachment and subsequent inhibition of proteins and molecules involved in the virus endocytosis [46,47]. The antiviral assay in this study evaluated the potential of the extracts to interfere with virus adsorption to cells. Reduction of DENV-CPE by *Scutellaria* and *L. alba* extracts suggests their flavonoids may block virus-cell membrane interactions. *In silico* analysis support this. We selected the envelope E protein of DENV, which plays an important role in the process that allows the virus to enter the cell [33]. Flavonoid glycosides from these extracts exhibited the strongest affinity for amino acids of the DII domain that interacts with receptors to promote viral entry into cells [33]. In addition, flavonoid aglycones bound to the βOG biding site, which has been established as a target for developing antivirals for dengue [48]. Numerous flavonoids have been identified as ligands for the DENV-E protein [11,49].

DENV uses a variety of cell receptors to gain entry into Vero cells [35–37]. The Gas6-Axl complex was selected for the *in silico* analysis. Flavonoid glycosides from anti-DENV active extracts showed good binding affinities to Gas6, suggesting potential biological interference with this receptor, whereas none of the flavonoid aglycones bound effectively. Flavonoid glycosides may have prevented DENV virions from adhering to Vero cells by blocking the PtdSer-Gas6 binding step. Disrupting the PtdSer-Gas6-Axl complex has been proposed as a potential therapeutic approach to inhibit DENV replication [36]. Flavonoids may also have entered the cells and affected the expression of Gas6 and Axl. Luteolin can downregulate the expression of these proteins in human cells [50].

Dynamin-dependent and clathrin-mediated endocytosis pathways are involved in DENV entry into Vero cells [33–35]. Targeting these pathways has been proposed as a strategy for developing antivirals [40,51]. The N-terminal domain (CTD) of clathrin and the GTPase domain of dynamin were selected for *in silico* analysis. Once again, flavonoid glycosides present in extracts with anti-DENV effect exhibited the best binding affinities with CTD and GTPase. Baicalein and scutellarin, abundant flavonoid aglycones in *Scutellaria* extracts, had the best binding affinity to both proteins. The flavonoids may have destabilized the W-box domain of clathrin-CTD and reduced the capacity of dynamin to exchange GDP for GTP. This, in turn, may have affected the functionality of both proteins, consequently impacting the endocytosis process of DENV in Vero cells. Also, it is plausible that the flavonoid treatment altered the fluidity of both the viral envelope and the cell membrane, thereby affecting their fusion process during virus endocytosis into the cell. The capacity of flavonoids to affect cell membrane fluidity (raft-breaking effect) has been documented [52].

4. Materials and Methods

4.1. Reagents

HPLC-grade acetonitrile, HPLC-grade formic acid (FA), isopropanol (98%), ammonium formate (AF, ≥99%), LC/MS-grade methanol, and potassium persulfate (≥98%) were obtained from Merck (Darmstadt, Germany). Standard substances (e.g., eriodictyol-7-glucoside, salvigenin, galangin, scutellarin, apigenin-7-glucuronide) were purchased from Sigma-Aldrich (St. Louis, MO, USA), Chemfaces (Wuhan, China) and Phytolab GmbH (Vestenbergsgreuth, Bavaria, Germany). MO, USA).

Type I water was obtained from a Millipore Direct-QTM purification system. Eagle's Minimum Essential Medium (MEM), fetal bovine serum (FBS), phosphate buffered saline (PBS), and antibiotics were purchased from Gibco (Grand Island, NY).

4.2. Viruses and Cell

Dengue virus type 1 (DENV-1) strain US/Hawaii/1944 and Dengue virus type-2 (DENV-2) New Guinea C strain (NGC) were used. Viruses were propagated titrated in BHK-21 cells as in a previous study [53]. African green monkey kidney (Vero) cell line (ATCC® CCL-81™) was cultured in Eagle's Minimum Essential Medium (EMEM) containing 10% fetal bovine serum (FBS, Gibco, NY, U.S.A.) at 37 °C in the presence of 5% CO₂.

4.3. Extracts

Plant material was provided by the Colombian government through Contract No. 270 for Access to Genetic Resources and Derived Products between the Ministry of Environment and Sustainable Development and the Industrial University of Santander. The plants used in this study were grown in the experimental plots at the Agroindustrial Pilot Complex of the National Center for Agroindustrialization of Aromatic and Medicinal Tropical Vegetables (CENIVAM) in the Industrial University of Santander (Bucaramanga, Colombia). The plants were dried in the dark, and leaves and stems were crushed and homogenized. Voucher specimens were deposited in the Herbarium of the Industrial University of Santander. Fourteen extracts were included in the analysis of their anti-DENV effect. Eight extracts were prepared in this study using the UAE technique following the protocol used in previous studies [20,22]. Briefly, dried leaves and stems (100 g) were crushed and the material was mixed with ethanol:water (20 mL; 70:30), the mixtures were subjected to ultrasonication (35 kHz, Elmasonic S15H, Singen, Germany) and filtered (Wattman No. 1 paper), and the residue was extracted again with ethanol:water (10 mL). Temperature of 50 °C for 60 min was used. The extracts were vacuum roto-evaporated in a Heidolph apparatus, dried in a VirTis AdVantage Plus tray lyophilizer, and stored at 4 °C in the absence of light. Six extracts were prepared in previous studies using UAE [20,22] or SFE techniques [21]. Each extract (1x10⁵ µg/mL) was dissolved in 1% dimethyl sulfoxide (DMSO) and stored at -20 °C before analysis.

4.4. UHPLC/ESI-Q-Orbitrap-MS Analysis

UHPLC-Q-Orbitrap-MS/MS analysis was used for identifying and characterizing the chemical components of the eight extracts prepared in this study, in accordance with the protocol used in a previous study [22]. An Ultimate Dionex™ 3000 UHPLC (Thermo Fisher Scientific, Bremen, Germany) connected to an Orbitrap™ mass detector Exactive Plus, Bremen, Germany), with heated electrospray ionization (HESI-II; Thermo Fisher Scientific), operated in positive-ion acquisition mode (350 °C). Chromatographic separation was performed on 50 mm L × 2.1 mm I.D. Zorbax Eclipse XDB C18 column, 1.8 µm particle size (Sigma-Aldrich, St. Louis, MO, USA). The mobile phase was a mixture of 0.2% formic acid-water (A) and 0.2% formic acid-acetonitrile (B) at a flow rate of 0.3 mL/min. The initial gradient condition was A-100%, which linearly changed to B-100% in 8 min, held for 4 min, returned to A-100% in 1 min, followed by 3 min of equilibration. The injection volume was 2 µL. Mass spectrometry experiments were accomplished on a Q-Exactive Plus Orbitrap mass spectrometer (Thermo Scientific, Bremen, Germany) connected to a the UHPLC and equipped with an electrospray ionization (ESI) source. Samples were analyzed in negative ion modes. The parameters were as follows: mass range, m/z 80 to 1000; electrospray ionization temperature, 350 °C; capillary temperature, 320 °C; capillary voltage, 3.5 kV; higher-energy-collisional dissociation cell (HCD), 10- 40 eV range. Data were analyzed using Thermo Scientific™ Dionex™ Chromatography Data System (CDS) software, version 7.2 and Thermo Xcalibur 3.1 software (Thermo Scientific, CA, USA). Extract metabolites were identified by comparing their retention times (tR), exact ion masses, isotopic ratios and fragmentation patterns with those of standard substances and databases [31,54].



All samples were run in triplicates and the data were presented as the mean value \pm standard deviation (SD) of mg per g of freeze-dried extract.

4.5. Crystal Violet Assays

The assay evaluated the effect of the fourteen extracts on the viability of non-DEN-infected Vero cells. Two different protocols, each including seven extract concentrations (3.12 to 250 μ g/mL), were followed. Protocol 1: cell monolayers were treated with extract for 1.5 h, the extract was removed by washing with PBS, fresh medium MEM with 2% fetal bovine serum was added, and the plates were incubated at 37 °C; 5% CO₂ for five days. Culture supernatants were discarded and crystal violet solution (0.05%) was added followed by methanol, and then the plates were then analyzed using an ELISA plate reader at a wavelength of 570 nm. Untreated cells and cells treated with DMSO were run in parallel as control negative and positive, respectively. The higher concentration of extract that did not reduce cell viability respect to untreated control was calculated by regression analysis (GraphPad Software, San Diego, CA, USA). Protocol 2: cell monolayers were incubated in culture medium containing extract for 72 h, the extract was then removed by washing, and the cell viability was measured as in Protocol 1. Untreated cells and cells treated with DMSO were included as controls. The CC₅₀ values were calculated by regression analysis as in previous studies [20,53].

4.6. Cytopathic Effect (CPE)-Based Antiviral Assay

Extracts were analyzed in the CPE-based antiviral assay according to the protocol used in a previous study [53]. DENV (1 PFU/cell) was adsorbed on Vero cells grown in 96-well plate for 1.5 h at 37 °C; 5% CO₂ in the presence of plant extract at non-cytotoxic concentrations (3.12 to 100 μ g/ml); then, the cells were washed with PBS and fresh media without extract was added to allow virus replication. After five days of incubation at 37 °C, the culture supernatant was discarded and cell viability measured using the crystal violet assay. Untreated DENV-infected cells and virus-infected / SDS-treated cells were included as negative and positive controls, respectively. DENV CPE (%) was calculated as follows: [(OD₅₇₀ of infected treated cells / OD₅₇₀ of uninfected untreated cells) \times 100]. DENV CPE reduction was calculated as follows: DENV CPE reduction (%) = [(OD₅₇₀ of infected treated cells - OD₅₇₀ of negative control) / (OD₅₇₀ of positive control - OD₅₇₀ of negative control) \times 100]. The concentration of extract that inhibited DENV-CPE by 50% (IC₅₀) was calculated by nonlinear regression followed by the construction of a concentration-response curve (GraphPad Prism software version 8.0, San Diego, CA, U.S.A.). Selectivity index (SI = CC₅₀ / IC₅₀) values were calculated. Each extract was analyzed in triplicate in three independent assays.

4.7. Molecular Docking Analysis

Three-dimensional structures of target proteins were downloaded from the Protein Data Bank. DENV-2 E protein (PDB ID: 10AN), Gas6-Axl receptor (PDB ID: 2C5D), clathrin (CDT domain, PDB ID: 2XZG), and dynamin (GTPase domain, PDB ID: 2X2E). Structures of flavonoids were retrieved from the PubChem (<https://pubchem.ncbi.nlm.nih.gov/> database (accessed on September 2024). The preparation of the target and ligands and molecular docking analyses were carried out using AutoDock Vina (Version 1.5.6, La Jolla, CA, USA), as described in previous studies [53,54]. The optimized protein structure was saved in the PDBQT file format. Default parameters were used, and the search exhaustiveness parameter was set to 100. Twenty five docked conformations were generated for each ligand using docking simulations. Three simulations were performed for each ligand–protein pair using seeds 6, 12, and 18. The ligand–protein interactions was displayed using the Discovery Studio Visualizer v21.1.0.20298 software.

4.8. Statistical Analysis

The relationship between antiviral activity and the flavonoid content was analyzed using two independent parameters: the chemical composition, represented as the absolute percentage (%) of

different flavonoid classes (Table 5), and the antiviral effect, DENV-CPE (%) as a unidimensional variable ranging from 0 to 100. The fourteen extracts were clustered based on their content of flavonoids and other compounds, using an unsupervised self-organized Kohonen Map [55]. One-way ANOVA and a Tukey-Kramer post hoc tests compared DENV-CPE (%) values between clusters, adopting a significance level of 0.05. The analysis was performed using the Matlab® R2021b software.

5. Conclusions

This study reports for the first time the correlation between the antiviral efficacy of extracts from medicinal plants cultivated in Colombia and their flavonoid content. Integration of antiviral assays, UHPLC analysis, and molecular docking analysis revealed that the content in flavonoid glycosides is a key determinant of the extracts' anti-DENV effect. Extracts rich in flavonoid glycosides, particularly flavones, demonstrated the greatest antiviral efficacy. In contrast, extracts with lower levels of glycosides or lacking them did not show antiviral activity. Docking analysis suggests that the flavonoids present in the extracts could block the interaction between DENV particles and the cell membrane via different mechanisms. Based on IC₅₀ and SI values from the CPE-based antiviral assay, the UAE-extract from *S. coccinea* can be classified as a prospective anti-DENV sample. This extract contains high concentrations of flavonoid glycosides with potential to inhibit DENV, and therefore could serve as a starting point for research on herbal medications for dengue treatment. Considerable evidence demonstrates the potential of *Scutellaria* species as an antiviral agent against various pathogenic viruses, including DENV.

Supplementary Materials: The following supporting information can be downloaded at the website of this paper posted on Preprints.org, Table S1: Amount (mg/g) of compounds in extracts reported in previous studies. Table S2: Docking score (kcal/mol) flavonoid ligands of DENV-2 (E) and Vero cell (Cl, clathrin; DY, dynamin; GA, Gas6-Axl complex) proteins.

Author Contributions: Conceptualization, R.E.O.; methodology S.A.V.; E.Q.-R.; software and data curation, S.C.-O.; E.E.S.; writing—original draft preparation, R.E.O.; S.A.V.; writing—review and editing, E.E.S. All authors have read and agreed to the published version of the manuscript.

Funding: The authors thank funding from the Ministry of Science, Technology and Innovation, the Ministry of Education, the Ministry of Industry, Commerce and Tourism, and ICETEX, Programme Ecosistema Científico-Colombia Científica, from the Francisco José de Caldas Fund; Grant RCFP44842-212-2018.

Institutional Review Board Statement: The Ministry of Environment and Sustainable Development of Colombia supported the Universidad Industrial de Santander through the permit to genetic resources and derivatives access for bioprospecting (Contract No 270). The project RC-FP44842-212-2018 was approved by the Scientific Research Ethical Committee (Record No. 15-2017, File No. 4110) from Universidad Industrial de Santander. The experiments and the chemical management were done according to national law (Resolution No 008430-1993) from the Ministry of Health of Colombia and the Institutional Manual of Integrated Management and Processes (PGOR-PGGA.05).

Informed Consent Statement: Not applicable.

Data Availability Statement: Not applicable.

Conflicts of Interest: The authors declare no conflict of interest.

References

- Wilder-Smith, A.; Ooi, EE.; Horstick, O.; Wills, B. Dengue. *The Lancet*. **2019**, 393, 350–363.
- Pan American Health Organization (PAHO). Dengue epidemiological situation in the region of the Americas, epidemiological week 35, 2025. PAHO: Washington, D.C., 2025. Available online: <https://www.paho.org/en/documents/dengue-epidemiological-situation-region-americas-epidemiological-week-35-2025> (accessed on 24 September 2025).

3. Obi, JO.; Gutiérrez-Barbosa, H.; Chua, JV.; Deredge, DJ. Current trends and limitations in dengue antiviral research. *Trop Med Infect Dis.* **2021**, *30*, 180.
4. Palanichamy Kala, M.; St John, AL.; Rathore, APS. Dengue: update on clinically relevant therapeutic strategies and vaccines. *Curr Treat Options Infect Dis.* **2023**, *15*, 27-52.
5. Rehman, B.; Ahmed, A.; Khan, S. et al. Exploring plant-based dengue therapeutics: from laboratory to clinic. *Trop Dis Travel Med Vaccines.* **2024**, *10*, 23.
6. Rajapakse, S.; de Silva, NL.; Weeratunga, P.; Rodrigo, C.; Sigera, C.; Fernando, SD. *Carica papaya* extract in dengue: a systematic review and meta-analysis. *BMC Complement Altern Med.* **2019**, *11*, 265.
7. Adeosun, WB.; Loots, DT. Medicinal Plants against Viral Infections: A Review of Metabolomics Evidence for the Antiviral Properties and Potentials in Plant Sources. *Viruses.* **2024**, *31*, 218.
8. Zhao, L.; Qian, S.; Wang, X.; Si, T.; Xu, J.; Wang, Z.; Sun, Q.; Yang, Y.; Rong, R. UPLC-Q-Exactive/MS based analysis explore the correlation between components variations and anti-influenza virus effect of four quantified extracts of *Chaihu Guizhi* decoction. *J Ethnopharmacol.* **2024**, *30*, 319, 117318.
9. Zhou, J.; Yuan, X.; Li, L.; Zhang, T.; Wang B. Comparison of different methods for extraction of *Cinnamomi ramulus*: yield, chemical composition and *in vitro* antiviral activities, *Nat. Prod. Res.* **2017**, *24*, 2909-2913.
10. Badshah, SL.; Faisal, S.; Muhammad, A.; Poulsom, BG.; Emwas, AH.; Jaremko, M. Antiviral activities of flavonoids. *Biomed Pharmacother.* **2021**, *140*, 111596.
11. Loaiza-Cano, V.; Monsalve-Escudero, LM.; Filho, CDSMB.; Martinez-Gutierrez, M.; Sousa, DP. Antiviral role of phenolic compounds against dengue virus: A Review. *Biomolecules.* **2020**, *24*, 11.
12. Shen, J.; Li, P.; Liu, S.; Liu, Q.; Li, Y.; Sun, Y.; He, C.; Xiao, P. Traditional uses, ten-years research progress on phytochemistry and pharmacology, and clinical studies of the genus *Scutellaria*. *J Ethnopharmacol.* **2021**, *30*, 265, 113198.
13. Huang, Q.; Wang, M.; Wang, M.; Lu, Y.; Wang, X.; Chen, X.; Yang, X.; Guo, H.; He, R.; Luo, Z. *Scutellaria baicalensis*: a promising natural source of antiviral compounds for the treatment of viral diseases. *Chin J Nat Med.* **2023**, *21*, 563-575.
14. Atkins S. Verbenaceae: the families and genera of fowering plants. Berlin: Springer; **2004**, *7*, 449–68.
15. Pascual, ME.; Slowing, K.; Carretero, E.; Mata, DS.; Villar, A. *Lippia*: traditional uses, chemistry and pharmacology: a review. *J Ethnopharmacol.* **2001**, *76*, 201–214.
16. Hennebelle, T.; Sahpaz, S.; Joseph, H.; Bailleul, F. Ethnopharmacology of *Lippia alba*. *J Ethnopharmacol.* **2008**, *5*, 116, 211-22.
17. Oliveira, DR.; Leitão, GG.; Fernandes, PD.; Leitão, SG. Ethnopharmacological studies of *Lippia origanoides*. *Revista Brasileira de Farmacognosia.* **2014**, *24*, 206-214.
18. Mamun-Or-Rashid, A. N. M.; Sen, M. K.; Jamal, M. A. H. M.; Nasrin, S. A comprehensive ethnopharmacological review on *Lippia alba* M. *Int. J Biomed. Mater. Res.* **2013**, *1*, 14-20.
19. Zandi, K.; Lim, TH.; Rahim, NA.; Shu, MH.; Teoh, BT.; Sam, SS.; Danlami, MB.; Tan, KK.; Abubakar, S. Extract of *Scutellaria baicalensis* inhibits dengue virus replication. *BMC Complement Altern Med.* **2013**, *29*, *13*, 91.
20. Quintero-Rueda, E.; Velandia, SA.; Ocazionez, RE.; Stashenko, EE.; Rondón-Villarreal, P. Comparative anti-dengue activities of ethanolic and supercritical extracts of *Lippia origanoides* Kunth: *in-vitro* and *in-silico* analyses. *Recs Nat Prod.* **2023**, *1*-18.
21. Arias, J.; Mejía, J.; Córdoba, Y.; Martínez, JR.; Stashenko, EE.; del Valle, JM. Optimization of flavonoids extraction from *Lippia graveolens* and *Lippia origanoides* chemotypes with ethanol-modified supercritical CO₂ after steam distillation, *Ind. Crops. and Prod.* **2020**, *146*, 112170.
22. Porras, SM.; Saavedra, RA.; Sierra, LJ.; González, RT.; Martínez, JR.; Stashenko, EE. Chemical characterization and determination of the antioxidant properties of phenolic compounds in three *Scutellaria* sp. plants grown in Colombia. *Molecules.* **2023**, *14*, *28*, 3474.
23. Quintero, WL.; Moreno, EM.; Pinto, SML.; Sanabria, SM.; Stashenko, E.; García, LT. Immunomodulatory, trypanocide, and antioxidant properties of essential oil fractions of *Lippia alba* (Verbenaceae). *BMC Complement Med Ther.* **2021**, *2*, *21*, 187.

24. Stashenko, EE.; Martínez, JR.; Cala, MP.; Durán, DC.; Caballero, D. Chromatographic and mass spectrometric characterization of essential oils and extracts from *Lippia* (Verbenaceae) aromatic plants. *J Sep Sci.* **2013**, *36*, 192-202.
25. Rodríguez-Morales, AJ.; López-Medina, E.; Arboleda, I.; Cardona-Ospina, JA.; Castellanos, JE.; Faccini-Martínez, ÁA.; Gallagher, E.; Hanley, R.; Lopez, P.; Mattar, S.; Pérez, CE.; Kastner, R.; Reynales, H.; Rosso, F.; Shen, J.; Villamil-Gómez, WE.; Fuquen, M. The epidemiological impact of dengue in Colombia: a systematic review. *Am J Trop Med Hyg.* **2024**, *29*, 112, 182-188.
26. Pájaro-González, Y.; Oliveros-Díaz, A.F.; Cabrera-Barraza, J.; CerraDominguez, J.; Díaz-Castillo, F. Chapter 1- A review of medicinal plants used as antimicrobials in Colombia. In: Chassagne, F. (Ed.). *Medicinal Plants as Anti-Infectives*. Academic Press. 2022; pp. 3–57.
27. Smee, DF.; Hurst, BL.; Evans, WJ.; Clyde, N.; Wright, S.; Peterson, C.; Jung, KH.; Day, CW. Evaluation of cell viability dyes in antiviral assays with RNA viruses that exhibit different cytopathogenic properties. *J Virol Methods.* **2017**, *246*, 51-57.
28. Gomes, AF.; Almeida, MP.; Leite, MF.; Schwaiger, S.; Stuppner, H.; Halabalaki, M.; Amaral, JG.; David, JM. Seasonal variation in the chemical composition of two chemotypes of *Lippia alba*. *Food Chem.* **2019**, *1*, 273, 186-193.
29. Lin, L.Z.; Mukhopadhyay, S.; Robbins, R.J.; Harnly, J.M. Identification and quantification of flavonoids of Mexican oregano (*Lippia graveolens*) by LC-DAD-ESI/MS analysis. *J. Food Compos. Anal.* **2007**, *20*, 361–369.
30. Parolin-Trindade, G.; Perez-Pinheiro, G.; Silva, AAR.; Porcari, AM.; Sawaya, ACHF. Sources of variation of the chemical composition of *Lippia origanoides* Kunth (Verbenaceae). *Nat Prod Res.* **2025**, *11*, 1-10.
31. The NIST Mass Spectrometry Data Center. The NIST Mass Spectral Search Program. Standard Reference Data Program of the National Institute of Standards and Technology, U.S.A.; National Institute of Standards and Technology: Gaithersburg, MD, USA, 2017. 66.
32. Timóteo, P.; Kariotia, A.; Leitão, SG.; Vincieri, FF.; Bilia, AR. HPLC/DAD/ESI-MS Analysis of non-volatile constituents of three Brazilian chemotypes of *Lippia alba* (Mill.) N. E. Brown. *Nat Prod Com.* **2008**, *3*, 12, 2017-2020.
33. Zhang, X.; Jia, R.; Shen, H.; Wang, M.; Yin, Z.; Cheng, A. Structures and functions of the envelope glycoprotein in flavivirus infections. *Viruses.* **2017**, *13*, 9, 338.
34. Meertens, L.; Carnec, X.; Lecoin, MP.; Ramdasi, R.; Guivel-Benhassine, F.; Lew, E.; Lemke, G.; Schwartz, O.; Amara, A. The TIM and TAM families of phosphatidylserine receptors mediate dengue virus entry. *Cell Host Microbe.* **2012**, *18*, 12, 544-57.
35. Cruz-Oliveira, C.; Freire, JM.; Conceição, TM.; Higa, LM.; Castanho, MA.; Da Poian, AT. Receptors and routes of dengue virus entry into the host cells. *FEMS Microbiol Rev.* **2015**, *39*, 155-70.
36. Piccini, LE.; Castilla, V.; Damonte, EB. Dengue-3 Virus Entry into Vero Cells: Role of Clathrin-Mediated Endocytosis in the Outcome of Infection. *PLoS One.* **2015**, *15*, 10, e0140824.
37. Acosta, EG.; Castilla, V.; Damonte, EB. Alternative infectious entry pathways for dengue virus serotypes into mammalian cells. *Cell Microbiol.* **2009**, *11*, 1533–1549.
38. Kirchhausen, T.; Owen, D.; Harrison, SC. Molecular structure, function, and dynamics of clathrin-mediated membrane traffic. *Cold Spring Harb Perspect Biol.* **2014**, *1*, 6, a016725.
39. Harper, C. B.; Popoff, M. R.; McCluskey, A.; Robinson, P. J.; Meunier, F. A. Targeting membrane trafficking in infection prophylaxis: dynamin inhibitors. *Trends in Cell Biology.* **2013**, *23*(2), 90–101.
40. Ho, MR.; Tsai, TT.; Chen, CL. *et al.* Blockade of dengue virus infection and viral cytotoxicity in neuronal cells *in vitro* and *in vivo* by targeting endocytic pathways. *Sci Rep.* **2017**, *7*, 6910.
41. Shen, L.; Pang, S.; Zhong, M.; Sun, Y.; Qayum, A.; Liu, Y.; Rashid, A.; Xu, B.; Liang, Q.; Ma, H.; Ren, X. A comprehensive review of ultrasonic assisted extraction (UAE) for bioactive components: Principles, advantages, equipment, and combined technologies. *Ultrason Sonochem.* **2023**, *101*, 106646.
42. Hou, M.; Hu, W.; Wang, A.; Xiu, Z.; Shi, Y.; Hao, K.; Sun, X.; Cao, D.; Lu, R.; Sun, J. Ultrasound-assisted extraction of total flavonoids from *Pteris cretica* L.: Process Optimization, HPLC Analysis, and Evaluation of Antioxidant Activity. *Antioxidants (Basel).* **2019**, *24*, 8, 425.
43. Uwineza, PA.; Waśkiewicz, A. Recent advances in supercritical fluid extraction of natural bioactive compounds from natural plant materials. *Molecules.* **2020**, *24*, 25, 3847.



44. Xiao, J. Dietary flavonoid aglycones and their glycosides: Which show better biological significance?. *Crit Rev Food Sci Nutr.* **2017**, *13*, 57, 1874–1905.
45. Moghaddam, E.; Teoh, BT.; Sam, SS.; Lani, R.; Hassandarvish, P.; Chik, Z.; Yueh, A.; Abubakar, S.; Zandi, K. Baicalin, a metabolite of baicalein with antiviral activity against dengue virus. *Sci Rep.* **2014**, *26*, 4, 5452.
46. Ortega, J.T.; Suárez, A.I.; Serrano, M.L. *et al.* The role of the glycosyl moiety of myricetin derivatives in anti-HIV-1 activity *in vitro*. *AIDS Res Ther.* **2017**, *14*, 57.
47. Pourfarzad, F.; Gheibi, N.; Namdar, P.; Gholamzadeh-Khoei, S.; Gheibi, N. Flavonoids antiviral effects: focusing on entry inhibition of influenza and coronavirus. *J Inflamm Dis.* **2024**, *28*, 1, e153347.
48. Naresh, P.; Selvaraj, A.; Shyam Sundar, P.; Murugesan, S.; Sathianarayananan, S.; Namboori P. K. K.; Jubie, S. Targeting a conserved pocket (n-octyl- β -D-glucoside) on the dengue virus envelope protein by small bioactive molecule inhibitors. *J. Biomol. Struct. Dyn.* **2022**, *40*, 4866–4878.
49. Waiba, A.; Phunyal, A.; Lamichhane, TR.; Ghimire, MP.; Nyaupane, H.; Phuyal, A.; *et al.* Computational insights into flavonoids inhibition of dengue virus envelope protein: ADMET profiling, molecular docking, dynamics, PCA, and end-state free energy calculations. *PLoS One.* **2025**, *20*, 7, e0327862.
50. Li, X.; Chen, M.; Lei, X.; Huang, M.; Ye, W.; Zhang, R.; Zhang, D. Luteolin inhibits angiogenesis by blocking Gas6/Axl signaling pathway. *Int J Oncol.* **2017**, *51*, 2, 677–685.
51. Alkafaas, SS.; Abdallah, AM.; Ghosh, S.; Loutfy, SA.; Elkafas, SS.; Abdel-Fattah, NF.; Hessien, M. Insight into the role of clathrin-mediated endocytosis inhibitors in SARS-CoV-2 infection. *Rev Med Virol.* **2023**, *33*, 1, e2403.
52. Kapral-Piotrowska, J.; Strawa, JW.; Jakimiuk, K.; Wiater, A.; Tomczyk, M.; Gruszecki, WI.; Pawlikowska-Pawłega, B. Investigation of the membrane localization and interaction of selected flavonoids by NMR and FTIR Spectroscopy. *Int J Mol Sci.* **2023**, *17*, 24, 20, 15275.
53. Silva-Trujillo, L.; Quintero-Rueda, E.; Stashenko, EE.; Conde-Ocacionez, S.; Rondón-Villarreal, P.; Ocacionez, RE. Essential Oils from Colombian Plants: Antiviral Potential against Dengue Virus Based on Chemical Composition, *In Vitro* and *In Silico* Analyses. *Molecules.* **2022**, *12*, 27, 6844.
54. Parra-Acevedo, V.; Ocacionez, R.E.; Stashenko, E.E.; Silva-Trujillo, L.; Rondón-Villarreal, P. Comparative virucidal activities of essential oils and alcohol-based solutions against enveloped virus surrogates: *in vitro* and *in silico* analyses. *Molecules* **2023**, *28*, 4156.
55. Kohonen, T.; Somervuo, P. How to make large self-organizing maps for nonvectorial data. *Neural Networks* **2002**, *15*, 945–952.

Disclaimer/Publisher's Note: The statements, opinions and data contained in all publications are solely those of the individual author(s) and contributor(s) and not of MDPI and/or the editor(s). MDPI and/or the editor(s) disclaim responsibility for any injury to people or property resulting from any ideas, methods, instructions or products referred to in the content.